Manganese Cluster in Photosynthesis: Where Plants Oxidize Water to Dioxygen

Vittal K. Yachandra,*,† Kenneth Sauer,*,†,‡ and Melvin P. Klein*,†

Structural Biology Division, Lawrence Berkeley National Laboratory, and Department of Chemistry, University of California, Berkeley, Berkeley, California 94720

Received April 8, 1996 (Revised Manuscript Received August 5, 1996)

Contents

I. Introduction 2927
II. Organization of Photosystem II 2929
III. Oxidation States of Mn in the Oxygen-Evolving Complex 2930
  A. Magnetic Resonance Spectroscopy 2930
    1. Electron Paramagnetic Resonance Spectroscopy (EPR) 2930
    2. NMR Proton Relaxation Studies 2931
    3. EPR Relaxation Studies 2932
  B. X-ray Absorption Near Edge Structure (XANES) 2932
  C. Electronic Absorption Spectroscopy 2934
IV. Structure of the Mn Cluster in the Oxygen-Evolving Complex (Mn-OEC) 2935
  A. Electron Paramagnetic Resonance 2935
  B. Extended X-ray Absorption Fine Structure 2936
    1. Structure of the Mn Complex 2936
    2. Evaluation of Models for the OEC 2938
  C. The Structural Role of the Cofactors Ca and Halide 2939
    1. Proximity of Ca to Mn 2939
    2. Is Chloride a Ligand of Mn? 2940
  D. Ligands of Mn 2941
V. Structural Changes During S-State Transitions 2941
  A. S_1 to S_2 State (Multiline EPR) Advance 2941
  B. S_1 to S_2 State ($g = 4.1$ EPR) Advance 2942
  C. NH_3- or F^--Modified S_2 State 2942
  D. S_0 State 2943
  E. S_2 to S_3 State Transition 2944
VI. Mechanism of Water Oxidation and O_2 Evolution 2945
VII. Conclusion 2948

I. Introduction

The essential involvement of manganese in photosynthetic water oxidation was implicit in the observation by Pirson in 1937 that plants and algae deprived of Mn in their growth medium lost the ability to evolve O_2.[1a] Addition of this essential element to the growth medium resulted in the restoration of water oxidation within 30 min. There is increased interest in the study of Mn in biological chemistry and dioxygen metabolism in the last two decades with the discovery of several Mn redox enzymes.[1b] The list of enzymes where Mn is required for redox activity includes a Mn superoxide dismutase, a binuclear Mn-containing catalase, a binuclear Mn-containing ribonucleotide reductase, a proposed binuclear Mn site in thiosulfate oxidase, a Mn peroxidase that is capable of oxidative degradation of lignin, and perhaps the most complex and important, the tetranuclear Mn-containing oxygen-evolving complex in photosystem II (Mn-OEC).[2] Mn is well suited for the redox role with accessible oxidation states of II, III, and IV, and possibly V: oxidation states that have all been proposed to explain the mechanisms of the Mn redox enzymes.

Most of the oxygen in the atmosphere which supports aerobic life on earth is generated by plants, algae, and cyanobacteria by the photoinduced oxidation of water to dioxygen:

$$2H_2O \xrightarrow{4h\nu} O_2 + 4e^- + 4H^+ \qquad (1)$$

Oxygenic photosynthesis that involves the oxidation of H_2O to O_2 by the Mn-OEC in the chloroplasts, and aerobic respiration that ultimately leads to reduction of O_2 to H_2O by cytochrome *c* oxidase in the mitochondria together form a cycle of dioxygen metabolism that is critical to both plant and animal life on earth.

Molecular oxygen is relatively abundant in the atmosphere primarily because of its constant regeneration by photosynthetic water oxidation by the Mn-OEC. The conversion of light energy into chemical potential is accomplished very efficiently by photosynthetic organisms. Higher plants, algae and cyanobacteria, in particular, are able to make use of water as an abundant raw material and oxidize it into molecular dioxygen, while producing reduced compounds with a reduction potential equivalent to that of molecular hydrogen. The reduced compounds produced by the carbon fixation reactions of photosynthesis have provided our major source of biological and fossil energy.

The oxygen-evolving complex (OEC) of the photosynthetic apparatus that catalyzes the reaction shown in eq 1 is thought to contain a cluster of four Mn atoms. The current phenomenological model of photosynthetic water oxidation involves five intermediate states, designated the S states.[3a] This is based on a remarkable phenomenon first observed by Joliot et al.;[3b] they found that the oxygen evolved when dark-adapted chloroplasts are excited by a series of short

* Authors to whom correspondence should be addressed.
† Lawrence Berkeley National Laboratory.
‡ Department of Chemistry, University of California, Berkeley.

S0009-2665(95)00052-5 CCC: $25.00

Vittal K. Yachandra was born in Masulipatnam, India, in 1953. He received his B.Sc. from Loyola College, University of Madras, India, in 1973, and a M.Sc. degree from the Indian Institute of Technology, Kanpur, India, in 1975. Subsequently, he moved to the United States and received a M.S. in chemistry from the University of Chicago in 1977, and a Ph.D. in chemistry from Princeton University in 1982 working on resonance Raman spectroscopy of iron–sulfur proteins and analogs, and X-ray absorption spectroscopy of Zn and Co carbonic anhydrase with Professor Thomas G. Spiro. He joined Lawrence Berkeley National Laboratory (LBNL) in 1982 as a postdoctoral fellow working with Professors Melvin Klein and Kenneth Sauer. Since 1985 he has been a Staff Scientist in the Structural Biology Division of LBNL. His main research interest has been the study of photosynthetic water oxidation and the structure and mechanism of the Mn–oxygen evolving complex by X-ray absorption, electron paramagnetic resonance, and vibrational spectroscopy. His other research interests include the application of X-ray absorption spectroscopy to low Z elements like sulfur and chlorine, especially ligand K-edge spectroscopy of sulfur in ferredoxins and related molecules to understand structural correlations with redox potentials.

Kenneth Sauer was born in Cleveland, OH, in 1931. After receiving his A.B. degree in chemistry at Oberlin College in 1953, he did his Ph.D. research on gas-phase photochemistry and the reactions of methylene with George Kistiakowsky at Harvard, finishing in 1957. He then spent three years as Assistant Professor of Chemistry at the American University of Beirut. In 1960 he went to the University of California, Berkeley, as a NIH postdoctoral fellow with Melvin Calvin, where he got his introduction to research in photosynthesis, which has been the underlying theme of his subsequent career. He joined the faculty of the Department of Chemistry at Berkeley in 1963 and was promoted to Professor in 1972. He has subsequently served as Vice-Chair of the Department of Chemistry and as Acting Associate Dean of the College of Chemistry. Since 1960 he has been an associate of the Lawrence Berkeley National Laboratory, currently as a member of the Structural Biology Division. In addition to the investigations of the mechanism of photosynthetic water oxidation described in this review article, his research includes studies of picosecond excitation transfer and trapping in pigment proteins containing chlorophylls and phycobilins, the consequences of electric fields generated during the initial electron transfer steps in the photosynthetic reaction centers and the dynamics of excited-state relaxation. He received the Research Award of the American Society for Photobiology in 1993 and has received fellowships from the Guggenheim Memorial Foundation and the Alexander von Humboldt Foundation.

Melvin Klein was born in Denver, CO, in 1921, attended the University of Colorado, received the A.B. in Physics in 1952 and the Ph.D. in Biophysics in 1958 for work in magnetic resonance from the University of California, Berkeley. He has been a staff member of the Lawrence Berkeley National Laboratory since 1952 and a senior staff member since 1962. Together with the late G. W. Barton, Jr., he devised the method of digital signal averaging for sensitivity enhancement. He has applied NMR and ESR to problems in biochemistry. With the advent of synchrotron radiation and the development of EXAFS he began the application of this method to the problem of determining the structure/function paradigm to the Mn cluster that is the catalytic site of photosynthetic water splitting/oxygen evolution. To permit study of the dilute Mn in the oxygen evolving complex, he developed the method of fluorescence detection of EXAFS. He has spent sabbatical leaves at the Bell Telephone Laboratories in 1961, as a Guggenheim Fellow at the École Polytechnique at Orsay, France in 1976, and at the Frei Universität Berlin and the Hahn-Meitner Institute as an Alexander von Humboldt Senior (U.S.) Scientist in 1988.

saturating flashes of light occurs in discrete pulses which exhibit a periodicity of four in amplitude. The first maximum yield of oxygen was observed following the third flash and thereafter following the seventh, eleventh, etc. flashes (Figure 1a). It was proposed by Kok[3a] that the OEC cycles through a series of five intermediate states (S_i, $i = 0-4$, representing the number of oxidizing equivalents stored on the OEC) driven by the energy of four successive photons absorbed by the pigment P_{680} of the photosystem II (PS II) reaction center. "Miss" or "double hit" parameters were proposed to explain the eventual damping of this four-flash periodicity. It was proposed that in the dark the complex relaxes to a predominantly S_1 population. Upon reaching the hypothesized S_4 state, the complex releases O_2 and returns to S_0 (Figure 1b).[3a] The tetranuclear Mn complex in the OEC is thought to couple the four-electron oxidation of water with the one-electron photochemistry occurring at the PS II reaction center by acting as the locus of charge accumulation and hence catalysis.

It is generally accepted that the Mn cluster is the active site for water oxidation, but the chemical mechanism by which this is achieved is inadequately understood. Additional cofactors Cl^- and Ca^{2+} are required for activity, but their exact structural and functional role is not yet clear.[4] The partially oxidized intermediates of the donor complex, the S states of the Mn-OEC (S_0-S_3), are stable on the time scale of many seconds to a few minutes, in contrast to the solution-phase products of serial one-electron oxidation of H_2O to O_2.[5] The structure and chemistry of the intermediates has been the subject of intense interest and study as has the structure of the Mn

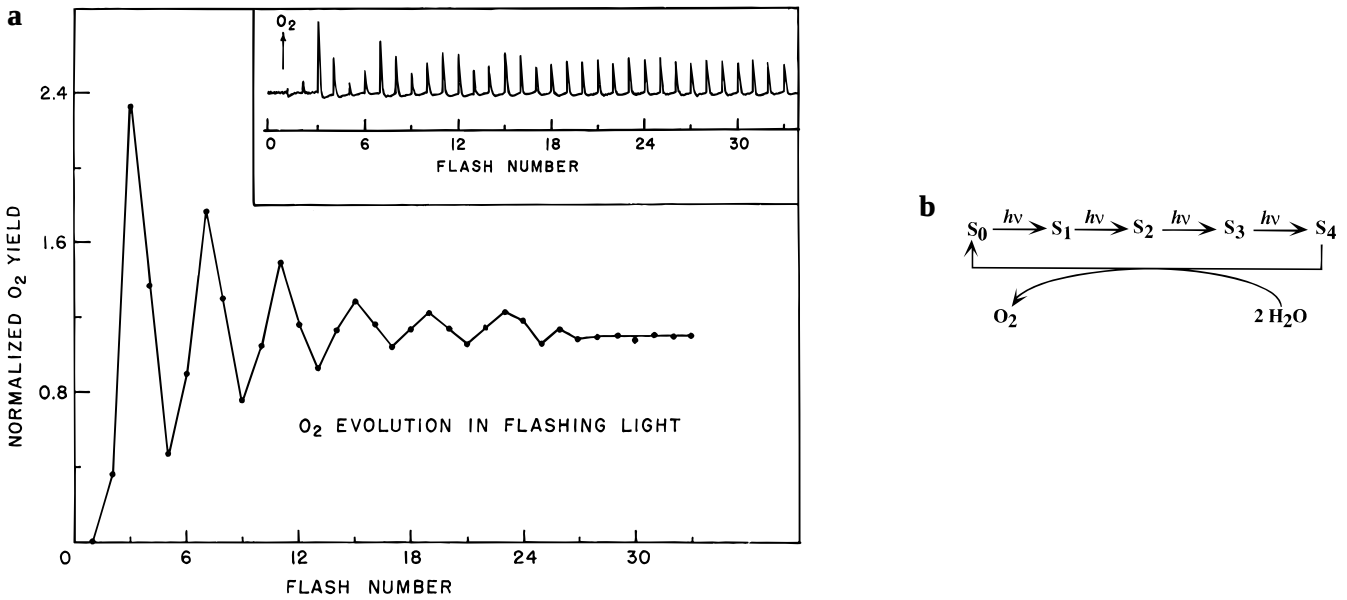

Figure 1. (a) The flash-induced pattern of oxygen evolution (reprinted from Babcock, G. T. Ph.D. Dissertation, University of California, Berkeley, CA, 1973; Lawrence Berkeley Laboratory Report 2172), and (b) the S-State scheme as proposed by Kok for the oxidation of water to dioxygen.[3a]

complex and its nuclearity, that is the number of Mn that are directly connected by bridging ligands. The proposed models include binuclear, trinuclear plus a mononuclear, and tetranuclear clusters.

Critical questions related to the process of photosynthetic water oxidation are: (1) What are the oxidation states and structural changes in the Mn complex as the OEC proceeds through the S-state cycle? And (2) what is the mechanism by which four electrons are removed from two water molecules by the Mn complex to produce an O_2 molecule? Electron paramagnetic resonance and X-ray absorption spectroscopy studies and the interplay between these two methods have provided significant insights into the structure and the mechanism of the OEC.[6] This review focuses on the application of these two methods that are Mn-specific spectroscopic techniques to resolve structural questions regarding the Mn cluster in the OEC. The emphasis is on the EPR and XAS work from our laboratory. More comprehensive surveys of the literature in the field of oxygen evolution are provided in the reviews by Babcock,[2e] Debus,[2a] and Rutherford et al.[2b] The EPR properties of the OEC are reviewed by Brudvig[7a] and by Vänngård et al.,[7b] the role of Ca and Cl by Yocum[4a,b] and Cl by Homann[4c] and Coleman,[4d] and the mechanistic aspects of photosynthetic oxidation by Renger[8a] and Govindjee.[8b] There are several excellent reviews focusing on the structural models of the Mn-OEC,[9a−d] the bioinorganic chemistry of Mn,[1b,9e] and its reactions with oxygen and its derivatives.[9f]

II. Organization of Photosystem II

Our understanding of the structure of PS II (Figure 2) has benefited from the crystal structure of the photosynthetic purple non-sulfur bacterial reaction centers.[10a] Portions of the D1 and D2 polypeptides that make up the core PS II complex have been shown to have significant homology with the corresponding portions of the L and M subunits of the

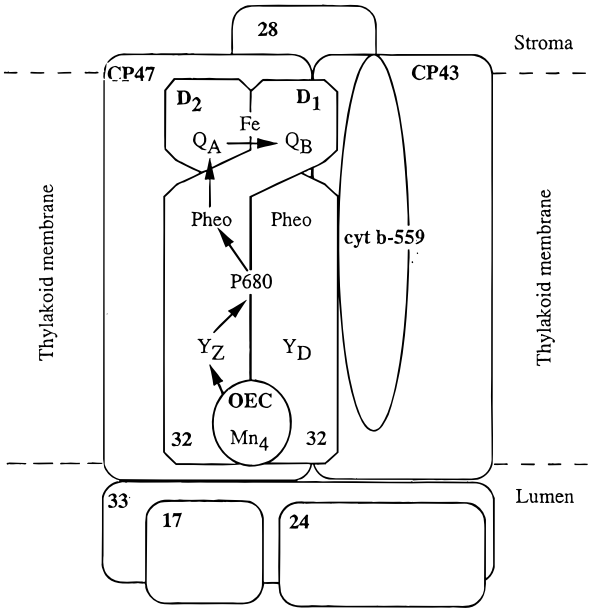

Figure 2. A structural model for the organization of the polypeptides of PS II in the thylakoid membranes. Solid arrows indicate the direction of electron transfer. P680 is the PS II reaction center. Electrons are transferred from the ultimate donor, the OEC, to the reaction center via the redox active tyrosine, Tyr_Z. Tyr_D is not involved in regular electron transport. The electrons are transferred from the reaction center to the pheophytin (Pheo) on the acceptor side, and then to the primary and secondary quinones Q_A and Q_B. D1 and D2 are the primary polypeptides. The groups, which are involved in electron transfer from the OEC on the donor side to the quinones on the acceptor side, mediated by the photochemistry occurring at the reaction center, are located in the D1 and D2 polypeptides. CP 47 and CP 43 are the chlorophyll-containing polypeptides, and the cyt b-559-containing polypeptide is a heterodimer of 4 and 9 kDa. The 17-, 24-, and 33-kDa extrinsic polypeptides are peripheral to the thylakoid membrane on the lumen side. (Adapted from ref 2a.)

bacterial reaction centers.[10b−e] In addition to the structural similarities, the kinetics and the EPR signals of the electron acceptor pathways have been

shown to be similar between the bacterial reaction center and PS II.[10f] This resemblance led to a construction of a working model (Figure 2) for the organization of the minimal unit of oxygen evolving PS II. On the electron donor side, the proposed model is more speculative because the electron-transfer components are different between the two systems, and the structural model of PS II does not benefit from the analogy to bacterial centers.

PS II is thought to consist of a reaction center similar to the structurally characterized center from the photosynthetic bacterial system, together with a donor complex that extracts electrons from water. The bacterial reaction center and the reaction center of PS II catalyze the light-dependent electron transfer from specialized chlorophyll pigment molecules, P_{870} and P_{680} in the bacterial and PS II reaction center respectively, to the primary quinone, Q_A, and subsequently to the secondary quinone, Q_B. The oxidized primary donor, P_{680} in PS II, is reduced by tyrosine Y_Z. Oxidized Y_Z, in turn, oxidizes the Mn-containing OEC that catalyzes the oxidation of water.

The minimal PS II preparation that retains oxygen evolution activity contains four Mn atoms, six major polypeptides, and one or more smaller polypeptides.[2a] Ca^{2+} and Cl^- are required for maximal oxygen evolution. The stoichiometry of four Mn atoms, one Ca, and one Cl per PS II is generally accepted to be required for oxygen evolution activity. The six essential intrinsic polypeptides are two polypeptides, D1 and D2, of about 32 kDa that contain the components involved in electron transfer from tyrosine Y_Z to the quinones Q_A and Q_B, including the reaction center P_{680}, CP47 and CP43, which contain chlorophyll and function as light harvesting antennae, and the 9 and 4 kDa polypeptides that coordinate the heme of the cyt *b*-559. There are three extrinsic polypeptides on the lumenal side, a 33 kDa polypeptide known as the Mn-stabilizing peptide that protects the Mn complex and maintains it in a configuration that optimizes the catalytic efficiency of water oxidation, and two other polypeptides of 24 and 17 kDa. The Mn complex is susceptible to attack by exogenous reductants when the 24 and 17 kDa polypeptides are removed. It is believed that the Mn complex is bound mainly to the intrinsic polypeptides, with the three extrinsic polypeptides conferring stability to the complex. Site-specific mutagenesis studies[11] have provided evidence for putative ligands for Mn on the D1 and D2 polypeptides, with many more on the D1 than on the D2 polypeptide.

The development of biochemical preparations that contained a purified PS II complex[12a,b] in the 1980s has had an enormous impact on the application of EPR and XAS methods to study the Mn complex. At present there are ever more refined preparations that have a smaller complement of polypeptides and still retain O_2 evolution activity.[13] PS II preparations from thermophilic cyanobacteria *Synechococcus* sp.,[14a] *Chlamydomonas*, and more recently, from cyanobacteria *Synechocystis* 6803[14b–d] have become available. These are the organisms of choice for site-specific mutagenesis and other molecular biological studies.[11]

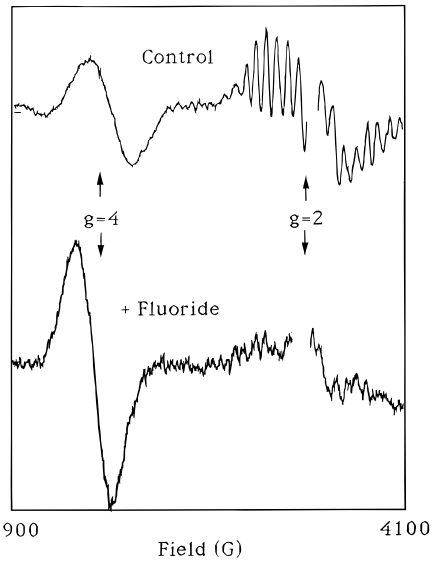

Figure 3. EPR signals associated with the oxygen-evolving center in spinach PS II preparations: The multiline EPR signal (shown on top) formed by advancement to the S_2 state following continuous illumination at 195 K: frequency, 9.2 GHz; temperature, 8 K; power, 30 mW; modulation amplitude, 32 G. The $g = 4.1$ EPR signal (shown at the bottom) produced by continuous illumination of a sample at 200 K in the presence of 20 mM fluoride; frequency, 9.2 GHz; temperature, 10 K; power, 50 mW; modulation amplitude, 32 G. The displayed EPR spectra result from the subtraction of background EPR spectra recorded prior to illumination.

III. Oxidation States of Mn in the Oxygen-Evolving Complex

A. Magnetic Resonance Spectroscopy

1. Electron Paramagnetic Resonance Spectroscopy (EPR)

The first direct spectroscopic evidence for the association of Mn with the S-state intermediates emerged from the discovery of a multiline EPR signal (MLS) centered at $g = 2$ with hyperfine structure characteristic of Mn (Figure 3).[15a] On the basis of its flash number dependence, the MLS was associated with the S_2 state. Similarity of this signal to the EPR spectra of a Mn_2(III,IV) complex with $S = {}^1/_2$ ground state[15b,e] led Dismukes et al. to propose a weakly exchange-coupled binuclear Mn_2(III,IV) or a $Mn_4(III_3,IV)$ tetranuclear structure,[15c] while Hansson and Andréasson found that a binuclear Mn_2(II,III) was in better agreement with their data.[15d]

A second EPR signal at $g = 4.1$ was subsequently discovered (Figure 3) and was tentatively assigned to a Mn species in the S_2 state.[16a,b] Upon annealing to a higher temperature of 195 K, this signal lost intensity while the MLS gained intensity. The origins of this signal were unclear for a considerable duration. One candidate for this signal was Fe^{3+}, because Fe^{3+} in a rhombic field exhibits signals in this region. Flash studies by Zimmermann and Rutherford[16c] provided experimental support to indicate that both the MLS and the $g = 4.1$ signal arise from different configurations of the light-induced S_2 state. On the basis of temperature dependence studies of the MLS and the $g = 4.1$ signal Hansson et al. suggested that the MLS arises from a binuclear

Mn_2(III,IV) species, while the $g = 4.1$ signal arises from a separate $S = {}^3/_2$ state of an axially distorted Mn(IV) monomeric species.[17a] Brudvig et al. proposed that both the $g = 4.1$ and multiline signals arise from different conformational states of a tetranuclear complex.[17b] Multifrequency EPR investigations (at 4, 9, and 16 GHz) have suggested that the $g = 4.1$ EPR signal arises from the middle Kramers doublet of a near rhombic $S = {}^5/_2$ system and favor a coupled multinuclear Mn complex.[17c] A noteworthy point is that despite a careful search in our laboratory at different conditions of temperature and power, the $g = 4.1$ signal has not been observed in PS II preparations from the cyanobacterium *Synechococcus*, although the MLS from *Synechococcus* is very similar to that observed from spinach preparations.[6b]

Treatment of PS II samples with F^- inhibits O_2 evolution. Illumination of samples so treated leads to a $g = 4.1$ EPR signal that is slightly different from that produced by controls (Figure 3).[16a]

Until recently EPR studies were limited to the S_2 state. If one electron is extracted during each S-state transition, then alternate S states should have an odd number of unpaired electrons and should in principle be detectable by EPR. No such signal has been observed for the S_0 state, which might be expected to be EPR active. An EPR signal has been discovered in Ca-depleted preparations[18a,b] and assigned by Boussac and Rutherford to a state equivalent to the S_3 state and was attributed to a histidine residue.[19] Recent ENDOR results[20] from Gilchrist et al. have shown the signal is from a stable tyrosine Y_Z^+ in Ca-depleted preparations. However, no such radical signal has been observed in native S_3-state samples.

The generally accepted interpretation of the S_2-state MLS signal is that it arises minimally from an $S = {}^1/_2$ antiferromagnetically exchange-coupled high-spin Mn_4(III,IV_3) species. The signal appears upon advancement from the S_1 state and correlates with a shift to higher X-ray energy of the Mn K-edge, indicating that this species occurs as $Mn_4(III_2,IV_2)$ in the S_1 state. The approach for detecting integer, non-Kramers spin transitions employs a microwave resonator in which the alternating magnetic field is parallel to the Zeeman field (parallel polarization mode) rather than the customary geometry in which the two fields are perpendicular. Using such an instrument configuration Dexheimer et al. observed an EPR signal (Figure 4) from samples in the S_1 state and concluded that this S_1 signal is a precursor to the MLS.[21a] A similar EPR signal has been reported by Dexheimer for a $Mn_4(III_2,IV_2)$ tetranuclear Mn complex.[21b] In contrast to this study Brudvig has postulated a diamagnetic ground state from measurements of the dipolar spin−lattice relaxation rates of tyrosine Y_D^+ in PS II samples subject to long-term dark adapatation.[22] Brudvig has postulated that the duration of dark adaptation has an influence on the properties of the S_1 state; short-term dark adaptation leading to an "active" form, while long-time dark adaptation results in a "resting" S_1 state. The differences in the EPR properties from the two studies may be related to the differences in the time of dark adaptation of the S_1-state samples.

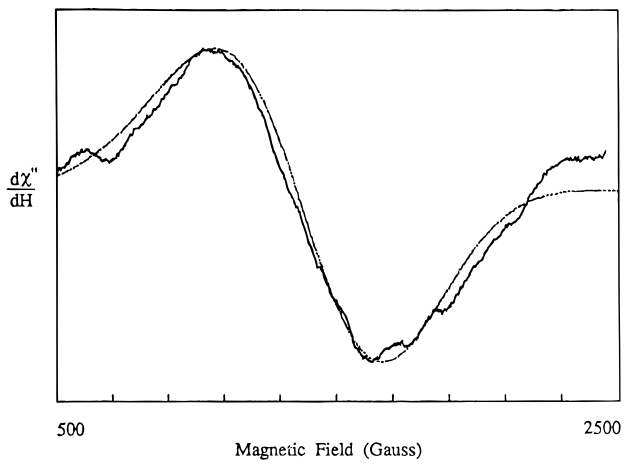

Figure 4. The parallel polarization EPR signal associated with the S_1 state of the OEC as observed in dark-adapted minus 200 K illuminated difference spectrum of a PS II preparation. The signal is at a g value of ~4.8 and ~600 G wide peak to peak. Spectrometer conditions: microwave frequency 9.2 GHz, microwave power 3 mW, temperature 4.2 K, field modulation 20 G at 100 kHz, scan time 4 min, time constant 2 s. The broken line displays the result of a computer simulation with parameters $S = 1$, $g = 2$, $D = -0.125$ cm^{-1}, $E = 0.025$ cm^{-1}. (Reprinted from ref 21a. Copyright 1992 American Chemical Society.)

2. NMR Proton Relaxation Studies

NMR relaxation rates of solvent protons are influenced greatly when the protons are in rapid exchange equilibrium with the coordination sphere of a paramagnetic metal ion. The relaxation rates of protons are enhanced several orders of magnitude by interaction with the unpaired electron spins on the paramagnetic metal ions. The relaxation times and rates of solvent water protons are very good markers for the properties of the paramagnetic metal ion.

NMR proton relaxation enhancement (NMR-PRE) methods have been used to study the Mn oxidation-state changes in the OEC. These experiments were carried out on flash-illuminated samples at a physiologically relevant temperature and are a direct probe of Mn in the S states. Among the Mn oxidation states, Mn(II) and Mn(IV) are candidates for strongly relaxing centers, while, Mn(III) is very weakly relaxing. Therefore exchanges occurring in the PRE after each S-state transition can be correlated with the redox state of the Mn.

The results from these studies in conjunction with the proposals from XANES and EPR results have led to the following model for Mn oxidation states:[23] (1) The proton relaxation rate increases upon formation of the S_2 state, indicating that one Mn(III) is oxidized to Mn(IV). (2) No change is observed in the PRE upon the formation of the S_3 state, implying no Mn oxidation accompanying the S_2 to S_3 transition. (3) The S_0 state is a fast relaxing state, indicating the presence of Mn(II). (4) Upon formation of the S_1 state, a slow relaxing state is produced, presumably because of oxidation of Mn(II) to Mn(III).

On the basis of the PRE results Sharp has proposed[23] that the Mn(IV) that is produced on the first flash is relatively isolated, although it is weakly coupled to the other three Mn atoms, and that it is

this Mn(IV) that is responsible for the $g = 4.1$ EPR signal in the S_2 state.

3. EPR Relaxation Studies

The spin−lattice relaxation time of the tyrosine radical Y_D^+ is accelerated by dipolar coupling to nearby paramagnets including the Mn complex. Relaxation enhancement has been observed in PS II preparations that lack Mn and has been attributed to the Fe that is associated with the electron acceptors in PS II. Much stronger enhancement is observed in the Mn-containing OEC, making it possible to separate the effects. The results from conventional power saturation[24a] and relaxation studies[24b] using pulsed EPR techniques lead to a model indicating (a) the absence of Mn oxidation upon S_3 formation, (b) the presence of a mixed-valence $S = {}^1/_2$ state not only in the S_2, in accordance with the observation of the multiline EPR signal, but also in the S_3 state, (c) an exchange-coupled, almost diamagnetic Mn cluster in the S_1 state, and (d) an $S = {}^1/_2$ Mn cluster containing Mn(II) in the S_0 state.

B. X-ray Absorption Near Edge Structure (XANES)

Questions concerning the oxidation states and symmetry of the Mn as a function of S-state have been addressed by examination of the X-ray absorption near-edge structure (XANES) at the Mn K-edge. The K-edge inflection energy of a first row transition element reflects principally the 1s → 4p transition energy for an isolated atom. However, in a metal complex containing ligands bonded to the metal, the assignment of the principal K-edge region and the near-edge region becomes very complicated; as yet there is no simple theoretical methodology available that provides a satisfactory explanation. Presumably the principal transition is from the 1s level of the metal to a molecular orbital with some p character. The position of the K-edge depends on the nature of the ligands; it has been determined that the metal atom with more electron-donating ligands is generally characterized by a lower inflection point energy. It has also been shown that the K-edge inflection point energy shifts to higher energies on increasing the oxidation state of the metal.[25a−c] These correlations permit an approximate oxidation state assignment for the metal when the nature of the ligands is known. A shift to higher energy results from an increase in the oxidation state of the metal complex, when it is known that there is no change in ligands. Despite these necessary reservations, important conclusions can be reached from X-ray edge studies.

Upon advance of the OEC from S_1 to S_2, the Mn K-edge of PS II shifts by 1.6−1.8 eV, which has been interpreted as evidence for direct Mn oxidation.[26a] Similar results were found for both PS II-enriched membrane preparations from spinach chloroplasts[26a] and for detergent-solubilized OEC preparations from the thermophilic cyanobacterium *Synechococcus* sp.[26b] A shift to higher energy was observed for the S_2 state generated by illumination at 190 K, or at 277 K in the presence of DCMU;[26c] both protocols limit the Mn-OEC to a one-electron turnover. This S_2 state is characterized by the multiline EPR signal. A similar shift was observed for samples advanced to the S_2 state by illumination at 140 K and characterized by the $g = 4.1$ EPR signal.[26d] The Mn K-edge spectra provided evidence that oxidation of Mn is associated with the induction of the $g = 4.1$ EPR signal. The Mn edge shift from the dark-adapted to the illuminated state of the F^--treated samples is similar to that of controls,[26e] showing again that formation of the $g = 4.1$ signal is associated with Mn oxidation.

Comparison of the inflection point energy and the edge shape with those from model compounds (Figure 5) is suggestive of an oxidation state of $Mn_4(III_2,IV_2)$ in the S_1 state[27] and $Mn_4(III,IV_3)$ in the S_2 state. This is in agreement with the observed EPR signals; S_1 being integer spin and therefore conventional EPR silent, and S_2 state being an exchange coupled Mn tetramer with a $S = {}^1/_2$ or ${}^5/_2$ ground state which results in the multiline EPR signal or the $g = 4.1$ signal, respectively. Ono et al.[28a] and Penner-Hahn et al., despite some earlier disagreements,[28b] presently concur with these assignments on the basis of their X-ray K-edge measurements.[28c]

It could be argued that structural changes and not oxidation-state changes are responsible for the K-edge energy shifts observed in PS II samples during the S_1 to S_2 transition. A comparison of several currently available multinuclear Mn complexes shows that even significant structural rearrangements do not result in the magnitude of edge shifts observed on oxidation state changes. Oxidation state changes in bi-, tri-, and tetranuclear complexes with the same or similar ligands and coordination environment result in Mn K-edge shifts of 1−2 eV.[6a] Significant changes in structure of complexes with identical oxidation states, such as replacement of a di-μ-oxo bridge by a mono-μ-oxo and μ-acetato bridges, result in inflection point energies that are different by only about 0.5−0.6 eV.[6a] Successive protonation of the oxo bridges in isostructural binuclear Mn(IV) complexes was shown to alter the magnetic coupling and the Mn−Mn distance without a significant change in the Mn X-ray absorption edge energies.[29]

Additional results were obtained on S_0- and S_3-like states, referred to as S_0* and S_3*, respectively, that were populated by low-temperature continuous illumination of chemically treated samples. It was possible to prepare samples with up to 65% of the centers in S_3 (the remaining fraction being in S_2) by this method. In the S_3* state the OEC was shown to have the same Mn K-edge position and shape as in S_2, suggesting the absence of direct Mn oxidation during the S_2-S_3 transition. It was proposed that the oxidation equivalent was stored on an amino acid residue.[30a] During the S_0 to S_1 transition Mn appears to become more oxidized, because the inflection energy of the S_1 state is ~2 eV higher than that in the S_0* state; it was suggested that the S_0 state contained Mn(II).[30b]

A promising approach to study the Mn oxidation states in the native S states is to step samples through the S-state cycle by the application of saturating single-turnover flashes and characterize these samples by XANES spectroscopy. Significant improvements in detection systems have made XAS

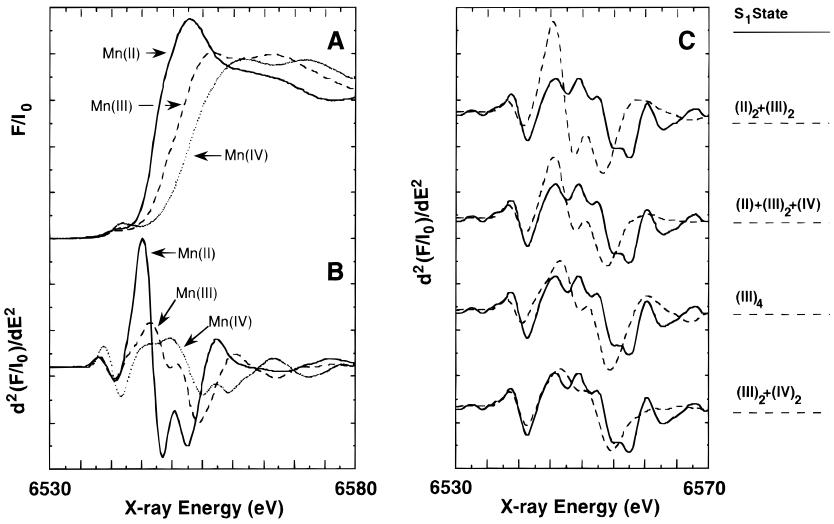

Figure 5. (A) The K-edge spectra of Mn(II), Mn(III), and Mn(IV) complexes and (B) their corresponding second derivatives. There is a significant change in shape as well as in inflection point energy as the oxidation state increases. The complexes are $Mn^{II}(acac)_2(H_2O)_2$, $Mn^{III}(acac)_3$, and $Mn^{IV}(sal)_2(bipy)$. (acac, acetylacetonate; bipy, bipyridine; and sal, salicylate). (C) The second derivative of the Mn K-edge of PS II particles in the S_1 state is shown as a solid line. Overplotted as dashed lines are the second derivatives of the Mn K-edge spectra created by weighted sums of spectra of the model complexes in different oxidation states (II), (III), or (IV) shown in B. The sets of oxidation states for the simulations were chosen to produce a conventional EPR-silent ground state. The particular combinations of oxidation states used in the simulations are shown at the right; the combination $(III)_2(IV)_2$ is the most similar to PS II in the S_1 state. (Reprinted from ref 46c. Copyright 1993 American Association for the Advancement of Science.)

experiments on samples in a single-flash saturable concentration regime possible. Mn XANES experiments on flash-induced S states have been reported.[28a] The occurrence of similar shifts in the edge position upon the first and second flash led those authors to conclude that direct Mn oxidation takes place during both the S_1 to S_2 and the S_2 to S_3 transitions. It was proposed that on each of the transients S_0-S_1, S_1-S_2, and S_2-S_3 Mn(III) was oxidized to Mn(IV). However, it is important to note that in these XANES studies no independent information was available on the actual S-state distributions in the samples used.

It is important to resolve the question of the assignment of the oxidation states of Mn, because it has an important bearing on the mode of charge accumulation on the Mn complex. If Mn is not oxidized during the S_2-S_3 transition, then one needs to invoke oxidation of a protein residue, a ligand of Mn, or substrate. Furthermore, the disappearance of the MLS EPR signal in the S_3 state samples needs to be rationalized (vide infra). As noted above, the MLS has provided the marker characteristic of the S_2 state. The loss of multiline signal intensity upon the S_2 to S_3 advance without apparent oxidation of manganese led Guiles et al. to the idea that oxidation of an alternative moiety might occur, and they proposed that a protein residue might play this role.[30a]

We now have XANES data of excellent quality from samples in the S_0 through S_3 states produced under physiologically relevant conditions.[31] We used light pulses from a Nd-YAG laser or from a Xe lamp to illuminate PS II samples at 277 K to achieve this objective. Because the actual S-state composition is of critical importance to the interpretation of the results, we characterized the samples by EPR spectroscopy, using the multiline EPR signal (MLS) as a direct measure for the amount of S_2 in our samples.

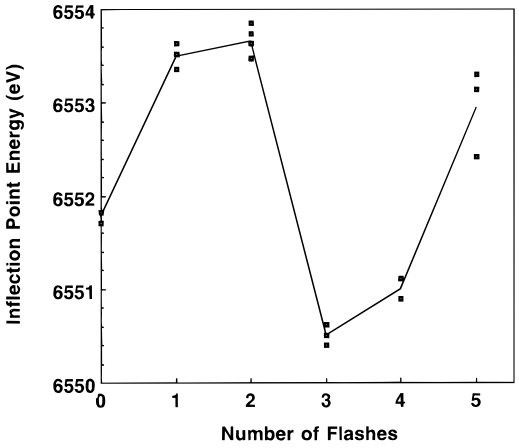

Figure 6. Inflection-point energy (IPE, in eV) of the Mn K-edge of PS II membranes as a function of the number of applied flashes. Shown are the IPE of 3−4 individual samples per flash number and their averages (—). (Reprinted from ref 31; copyright 1996 National Academy of Sciences, USA.)

The relative S-state populations in samples given 0, 1, 2, 3, 4, or 5 flashes were determined from fitting the flash-induced EPR-multiline signal oscillation pattern to the Kok S-state kinetic model in each of the samples used in the XAS experiment. Our edge data are of sufficient *S/N* quality to permit not only a determination of the absorption edge position (the inflection point energy, defined as the zero-crossing in the second derivative of the edge), but also an analysis of the structure of the edge as a function of the number of flashes.

Figure 6 shows the Mn K-edge inflection point energies as a function of flash number. The edge spectra of samples exposed to 0, 1, 2, or 3 flashes were combined with EPR information to calculate the *pure* S-state edge spectra (Figure 7). The edge positions (defined as the zero-crossing of the second deriva-

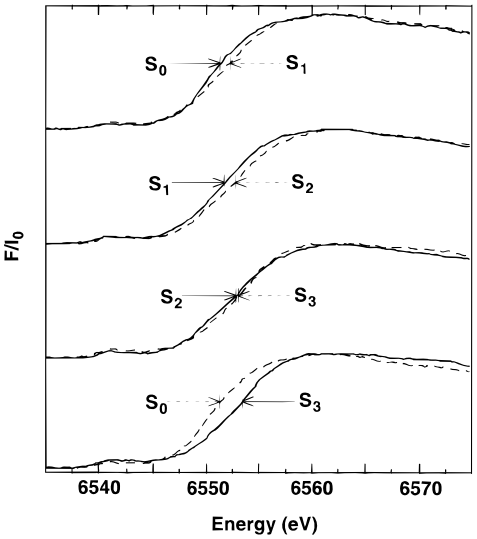

Figure 7. Normalized Mn K-edge spectra for the pure S states of the Mn cluster of PS II, as calculated from the flash-induced edge spectra of samples given 0, 1, 2 or 3 flashes. These are the averages of the S-state spectra extracted from three different groups of samples; each group contains 2−4 sets of samples given 0−3 flashes. A linear scatter background was subtracted, and the spectra were normalized at the energy of maximal absorption. To emphasize the changes during the various S-state transitions, the spectra of successive S-states are overlaid. (Reprinted from ref 31. Copyright 1996 National Academy of Sciences, USA.)

tives) are 6550.1, 6551.7, 6553.5, and 6553.8 eV for S_0, S_1, S_2, and S_3, respectively. Each of the S_0 to S_1 and the S_1 to S_2 transitions is accompanied by a shift of the edge to higher energies by ca. 1.6−1.8 eV, indicating that during those transitions the Mn cluster undergoes oxidation. The S_2 to S_3 transition, however, leads to an edge shift of only 0.3 eV, consistent with the absence of a direct Mn oxidation step. These interpretations are supported by the data on model compounds (see above). This is suggestive that the observed edge shift during the S_2 to S_3 transition is caused more likely by a change in the ligand environment of the Mn cluster and/or ligand oxidation than by direct Mn oxidation.

In addition to the shift in edge position, the S_0 to S_1 and S_1 to S_2 transitions are accompanied by characteristic changes in the shape of the edge, also indicative of Mn oxidation. The shape of the Mn edge is informative with regard to changes of the oxidation state of the Mn cluster. We showed previously that the spectral region around the inflection point, between 6545 and 6555 eV, reflects predominantly oxidation-state changes, whereas the region between 6555 and 6575 eV reflects changes in the coordination environment of the Mn.[27] In Figure 8 we show the second derivatives of the normalized S-state edge spectra. Several features change reproducibly with S state. During the S_1 to S_2 transition a pronounced positive feature appears at 6552 eV, marked with **a**, whereas above 6555 eV the edge remains virtually unchanged. The shape of the edge in the spectral range between 6545 and 6555 eV (highlighted in the S_3 spectrum in Figure 8) remains mostly unchanged at the S_2 to S_3 transition. In the lower panel of Figure 8 the second derivatives of some typical edge spectra of tetranuclear Mn compounds in oxidation

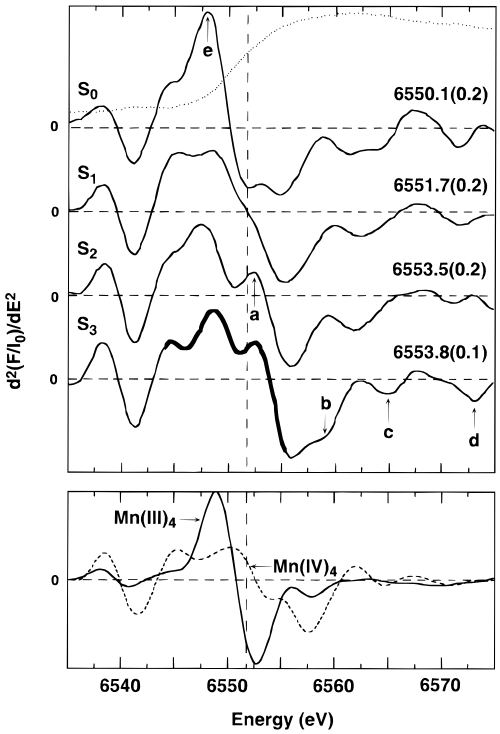

Figure 8. Upper panel: second derivatives of the normalized pure S-state edge spectra of the Mn cluster of PS II. For clarity a vertical dashed line has been drawn at the inflection-point energy (IPE) of the S_1 state. The IPE (in eV) for each S state is given at the right, and the number in parentheses is the standard deviation. Lower panel: second derivatives of the normalized Mn K-edge spectra of $Mn^{III}_4(\mu_3\text{-}O)_2(AcO)_7(2,2'\text{-bipyridine})(ClO_4)$ (solid line), and $Mn^{IV}_4(\mu_2\text{-}O)_6(1,4,7\text{-triazacyclononane})_3(ClO_4)_4$ (dashed line). (Reprinted from ref 31. Copyright 1996 National Academy of Sciences, USA.) Mn complexes were provided by Profs. G. Christou, K. Wieghardt, and W. H. Armstrong.

states III and IV are shown. The shape of the edge between 6545 and 6555 eV better supports a model for the Mn cluster containing at least one Mn(III), rather than being all Mn(IV). Reproducible changes in shape are observed between 6555 and 6575 eV for the S_2 and S_3 states (indicated with **b**, **c**, and **d**). These results suggest that changes occur in the coordination environment of the Mn, rather than in the oxidation state of the Mn. The spectrum of the S_0-state completely lacks feature **a** around 6552 eV. A positive feature around 6548 eV (marked **e**) is present, having a much larger amplitude and a significantly narrower width than that in the S_1 spectrum. This intense and narrow feature is suggestive of the presence of Mn(II) or a greater amount of Mn(III) in the complex (see Figure 5B).

The proposed Mn oxidation state assignments are as follows: S_0 (II,III,IV,IV) or (III,III,III,IV); S_1 (III,-III,IV,IV); S_2 (III,IV,IV,IV); S_3 (III,IV,IV,IV)$^{\bullet}$ (Figure 9). No EPR signals have yet been detected from the S_3 or the S_0 state, although, one could expect an EPR signal from either of the oxidation state assignments for each of these S states.

C. Electronic Absorption Spectroscopy

Extracting electronic absorption spectra related to the Mn cluster from the absorption of the many Chl molecules contributing to the PS II spectrum and

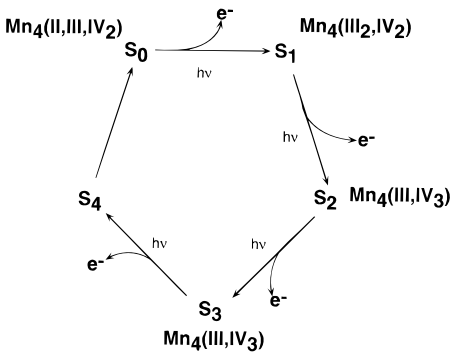

Figure 9. Summary of the oxidation states of Mn in the S-state cycle. The oxidation state of Mn does not change at the S_2 to S_3 transition. The oxidation equivalent produced during the S_2-S_3 transition is proposed to be delocalized over the $Mn_2(\mu\text{-oxo})_2$ bridged unit in the S_3 state (see text for details).

deconvolving the changes occurring on the acceptor side has been difficult at best. For a comprehensive review the reader is referred to the article by Dekker.[32a] The consensus from these studies is that there is oxidation of Mn(III) to Mn(IV) in the S_1 to S_2 transition and that the S_0 to S_1 transition involves Mn(II) to Mn(III) oxidation. The assignment of the Mn oxidation during the S_2 to S_3 transition was not resolved. Recently, Junge and co-workers have monitored nano- to millisecond absorption transients from the near UV into the near-IR spectral regions of Cl^--depleted PS II samples.[32b] These data support the interpretation that the oxidizing equivalents produced during the S_0 to S_1 and S_1 to S_2 transitions are stored on the Mn complex, and the oxidizing equivalent produced during the subsequent S_2 to S_3 transition resides on an as yet unidentified chemical species; tentatively assigned as a His residue.

IV. Structure of the Mn Cluster in the Oxygen-Evolving Complex (Mn-OEC)

Structural information about the Mn complex is derived mainly from two methods, EPR and X-ray absorption spectroscopies. It is important for models derived from both these methods, especially XAS methods, to know the number of Mn atoms present in the OEC. Despite some controversy in the literature, it is generally agreed that there are four Mn atoms per PS II.

A. Electron Paramagnetic Resonance

The synthesis and structure determination of the di-μ-oxo Mn_2(III,IV) bipyridine by Plaksin et al.[15e] provided a molecule with significant consequences. The observation and assignment of its 16-line EPR spectrum by Cooper et al.[15b] provided an immediate guide to Dismukes and Siderer[15a] when they subsequently observed the now famous multiline EPR signal that is the hallmark of the S_2 state. This signal provided the first evidence for a multinuclear form of the manganese complex. In contrast to the 16 hyperfine lines resulting from the antiferromagnetically coupled Mn_2(III,IV) bipyridyl complex, the S_2-state multiline signal extends over a broader field range and exhibits at least 19 resolved hyperfine lines, with an average splitting of ~80 G. The increased number of hyperfine lines led Dismukes to propose that the spectrum could be modeled by either a binuclear or a tetranuclear complex.[15c]

Early temperature dependence studies assigned an excited-state origin for the MLS, thus predicating a larger than binuclear Mn cluster.[33a] Despite some controversy regarding the temperature dependence of the MLS signals it is now clearly established that the MLS [33b,c] is a ground-state signal.

The discovery of the $g = 4.1$ EPR signal from the S_2 state[16a,b] and, importantly, the recent observation of ^{55}Mn hyperfine structure[34a,b] have contributed significantly to the present consensus that the four Mn atoms are magnetically coupled and form a tetranuclear complex. The pathway leading to this consensus has traversed an interesting series of proposals to explain the origin of both of the EPR signals. It was initially proposed by Hansson et al. that the MLS could arise from a bi- or trinuclear cluster, and the $g = 4.1$ was assigned to a ground state $S = {}^3/_2$ mononuclear Mn(IV) complex.[17a] There are several examples of Mn(IV) $S = {}^3/_2$ systems giving rise to EPR signals in the $g = 4$ region of the spectrum. Conversion of the $g = 4.1$ form to the MLS form upon increasing the temperature was attributed to electron transfer from the multinuclear cluster to the mononuclear Mn. The observation of the MLS or the $g = 4.1$ in the presence of different cryoprotectants and inhibitors was explained as due to modulation of the redox equilibrium between the two forms.[17a]

An alternative proposal assigned the MLS and $g = 4.1$ signals as arising from different spin states of the same Mn cluster.[17b] Preferential population of the spin states was explained by invoking a conformational change that was dependent on temperature, cryoprotectants, or inhibitors. The most recent denouement of the relation of the MLS and the $g = 4.1$ signal has come from the observation that at around 150 K the state responsible for the MLS is converted to that responsible for the $g = 4.1$ signal upon the absorption of infra red light around 820 nm.[35] It is suggested that the conversion of the MLS to the $g = 4.1$ signal results from the absorption of infrared light by the Mn cluster itself, probably an intervalence charge-transfer band, resulting in electron transfer from Mn(III) to Mn(IV). The authors argue that therefore there is no reason to consider the state responsible for the $g = 4.1$ signal as a precursor of that which gives rise to the MLS.

The observation of at least 16 hyperfine lines in the $g = 4.1$ signal characteristic of Mn from spatially oriented ammonia-treated membranes (Figure 10) has provided definitive evidence for a Mn complex that it is at least a trinuclear cluster.[34a,b] A $S = {}^3/_2$ or ${}^5/_2$ ground state was proposed to be the origin of the $g = 4.1$ signal; either state can be explained to arise minimally from only a trinuclear Mn cluster. These studies have shown that it is unnecessary to invoke a mononuclear Mn(IV) to explain the $g = 4.1$ signal and that both of the EPR signals arise from the same Mn cluster that is minimally trinuclear. The multifrequency EPR data from Haddy et al.[17c] favor a $S = {}^5/_2$ spin state for the $g = 4.1$ signal, which is incompatible with a mononuclear Mn(IV) origin for

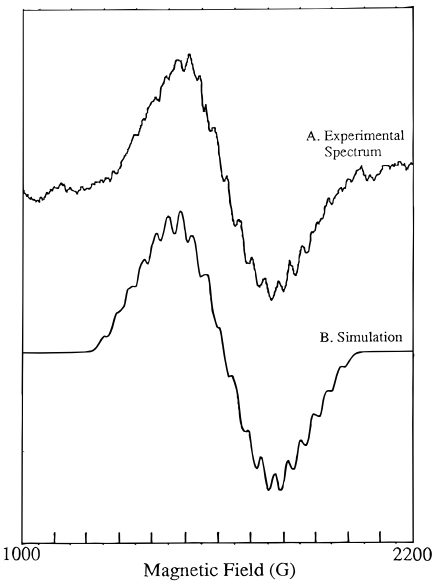

Figure 10. EPR spectrum of oriented PS II membranes with 100 mM NH_4Cl at pH 7.5 in the presence of 400 mM sucrose (A). The membrane normal is oriented parallel to the applied magnetic field (0°). The dark S_1-state spectrum has been subtracted from the S_2-state EPR signal recorded following 5 min illumination at 195 K. Spectrometer conditions: microwave frequency, 9.22 GHz; microwave power, 20 mW; field modulation amplitude, 10 G; sample temperature, 8 K. (B) Simulation of the spectrum in utilizing an effective $S' = {}^1/_2$ system and Gaussian line shapes. The following isotropic parameters were used: $g = 4.1$; $D_{hwhm} = 16$ G; $|A_1| = 47$ G, $|A_2| = 37$ G, $|A_3| = 34$ G, $|A_4| = 16$ G. The reduced hyperfine couplings are consistent with an $S = {}^3/_2$ or $S = {}^5/_2$ spin state of a Mn tetranuclear structure. (Reprinted from ref 34b. Copyright 1992 American Chemical Society.)

the signal. On the basis of their X- and Q-band results and temperature dependence of the signals at X-band, Smith and Pace[34c] argue for an isolated Mn_2(III,IV) species as the origin for the $S = {}^1/_2$ ground state MLS and an excited state origin for the signals they have observed at $g = 4.25$ and 6. They also report another EPR signal at $g = 3.98$ with an $S = {}^3/_2$ ground-state origin, and it is proposed to be from a Mn pair interacting with an oxidized protein side chain, possibly histidine.

Simulations of the MLS assuming a tetranuclear form of the cluster approximate the signal reasonably well.[36a−c] Theoretical analyses by Bonvoisin et al.[36a] led to the conclusion that a tetranuclear form of the cluster is essential to produce a MLS extending over a range of more than 1500 G. Trinuclear complexes lead to narrower spectra. The simulations of Zheng and Dismukes[36b] are based on exchange coupled $Mn^{III}-Mn^{IV}$, where the Mn(III) are all five coordinate, with the unpaired electron in an unusual $d_{x^2-y^2}$ ground state. Recent simulations based on multifrequency EPR by Ahrling and Pace have shown that the MLS features could be explained in terms of a magnetically isolated Mn_2(III,IV) binuclear cluster.[36d] These simulations require large quadrupolar couplings: to explain the large magnitude of these couplings it was proposed that the Mn are five coordinate or have a weakly bound sixth ligand. None of the simulations published thus far take into account the substructure that we and others have observed on each of the hyperfine lines of the MLS.[37a] It has been suggested that this substructure may arise from ligand superfine interaction, from quadrupole interactions of the Mn nuclei, or from unresolved hyperfine interaction from Mn. On the basis of S-band studies, Haddy et al.[37b] ascribe the additional lines to Mn hyperfine coupling.

Recently, Britt and co-workers have published ^{55}Mn ENDOR data and have presented simulations to binuclear, trinuclear, or tetranuclear clusters using parameters reported by other groups. The added constraints imposed on the simulations by the ENDOR data show that the best fits are obtained for the magnetically interacting tetranuclear cluster.[38]

B. Extended X-ray Absorption Fine Structure

X-ray absorption spectroscopy is particularly suited for the study of the Mn complex in PS II. X-ray absorption spectroscopy on PS II preparations involves measurements of the fluorescence-detected X-ray absorption spectrum with excitation energies at and above the Mn K-edge. Due to the selective excitation and detection of the Mn X-ray fluorescence, this technique allows investigation of the Mn complex without interference from pigment molecules, the lipid and protein matrix, or other metals such as Ca, Mg, or Fe, which are present in oxygen evolving PS II preparations. The Mn K-edge and preedge spectra provide information about the oxidation states (see above) and the site symmetry of the Mn complex. The extended X-ray absorption fine structure (EXAFS) results from interactions between the absorber Mn atom and the backscattering from ligand and neighboring atoms of Mn. EXAFS spectra provide information about the numbers, types, and distances of the backscattering atoms from the absorbing Mn atoms.[39]

EXAFS data provide a composite measure of the coordination of all the Mn atoms in the system: therefore, it is crucially dependent on the stoichiometry of Mn/PS II and the purity of the preparations. The interpretation of the data and the models that are plausible is based on the determination of four Mn/PS II. Although interpretations involving different numbers of Mn/PS II have been reported, the consensus number is four Mn/PS II, and most of the EXAFS data have been interpreted on that basis. Despite these caveats inherent to the method, EXAFS analysis has provided important insights into the structure of the Mn complex in the OEC and the changes that the Mn complex undergoes on advancement from the S_0 through the S_3 states.

1. Structure of the Mn Complex

The most significant breakthrough in the determination of the structure of the Mn complex came with the detection of the 2.7 Å Mn−Mn distance.[40] This distance was initially observed in broken, washed chloroplast samples. Through the development of the BBY procedure that permitted the isolation of PS II preparations that contained only the complement of four Mn/PS II required for oxygen evolution,[12a] it became possible to observe XAS with considerably increased S/N because of the absolute enrichment of Mn (Figure 11).[41] EXAFS techniques cannot distinguish between backscattering from Mn or Fe, the

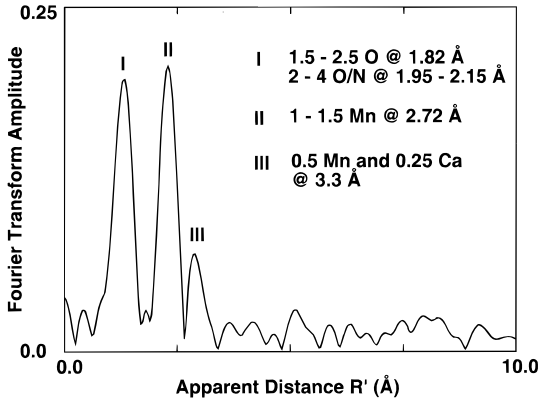

Figure 11. The Fourier transforms of the k^3-weighted Mn EXAFS data (3.5−12.0 $Å^{-1}$) from *Synechococcus* in the S_1 state. Note that the apparent distance *R′* in the transforms is shorter than the actual distance to a given neighboring atom due to the effect of the averaged phase of the EXAFS wave. (Reprinted from ref 46c. Copyright 1993 American Association for the Advancement of Science.)

other transition metal that is present in PS II preparations. However, Fe has not been implicated as part of the catalytic site for O_2 evolution. Hence, it is reasonable to assign the backscattering at 2.7 Å to Mn.

A series of papers also reported Mn−O interactions at ∼1.8 Å and an additional highly disordered shell of light atom (O, N) scatterers between 1.9−2.2 Å,[26b,c,30a,b,42] with a predominance of shorter distances around 1.9−2.0 Å.[26e] Similar results were found for PS II preparations both from spinach (BBYs) and from the thermophilic cyanobacterium *Synechococcus* sp.[26e]

Bridging Mn−O distances are typically about 1.8 Å in the multinuclear μ_2 or μ_3 oxo-bridged Mn complexes.[43] Comparison to multinuclear Mn complexes shows that a large distribution of distances is typical of Mn−O- or −N-terminal ligand distances. In compounds containing Mn(III) and Mn(IV), the distances range from 1.9−2.2 Å, depending on the oxidation state and type of ligand. Mn-terminal ligand distances for N-donor ligands are on average slightly longer than Mn−O distances for carboxylate or water ligands. The observed average of 1.9−2.0 Å distances favors the presence of more O than N-terminal ligands in the OEC. This is consistent with results from EPR and ESEEM experiments that suggest a dominance of carboxylate-derived ligands of Mn in the protein.[6b]

Examination of a series of multinuclear Mn complexes reveals that the Mn−Mn distances[44] range between 2.6 and 2.8 Å in complexes where two Mn atoms are bridged by at least two μ_2-oxo, or two μ_3-oxo bridges. (An additional μ_2-acetate bridge is also present in some of these complexes.) In the complexes that contain the μ_3-oxo bridges there is also a Mn−Mn distance >3 Å, as illustrated in Figure 12. The distance decreases to 2.3 Å when the two Mn atoms are linked by three μ_2-oxo bridges.

The important point is that *at least two* μ-oxo bridges exist between pairs of Mn atoms in all reported complexes that have a Mn−Mn distance of about 2.7 Å. The quantitation of the Fourier peak at 2.7 Å leads to 1.2 ± 0.2 Mn scatterers per Mn in PS II at that distance. Therefore it was proposed

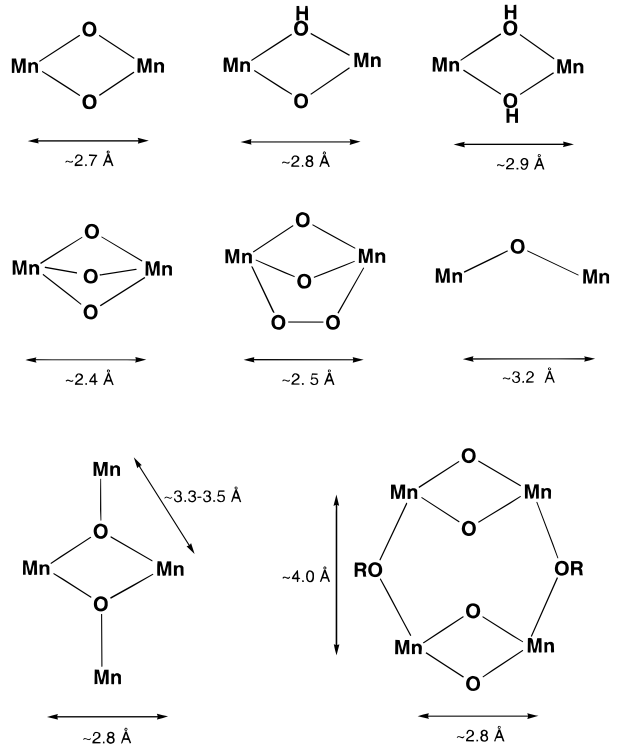

Figure 12. Different bridging structures and the respective Mn−Mn distances in some multinuclear Mn complexes.[1b,9,43,44,48]

that the Mn complex in the OEC is a structure with *minimally* two di-μ-oxo bridges. This conclusion was based principally on the observation of the 2.7 Å Mn−Mn distance, but it was also supported by the presence of the Mn−O distance at about 1.8 Å, which is characteristic of the bridging Mn−oxo distance in multinuclear Mn complexes.

In EXAFS studies, the detection and analysis of metal scatterers at distances greater than 3 Å can be difficult, owing to the combined effects of enhanced disorder, interference from other ligands, and the $1/R^2$ dependence of scattering amplitude.[45] Evidence for such an interaction was not reported consistently in the above EXAFS studies, leading to a prediction that the binuclear Mn units in the OEC were separated by >3 Å. More recent EXAFS studies of Mn in the OEC, at substantially lower sample temperatures and with improved signal to noise ratio,[28b,46a,b] have provided evidence for scatterers at >3 Å in addition to the interaction at 2.7 Å. These experiments include various combinations of oxygen-evolving preparations and EXAFS analysis techniques, and the interpretations differ. Our data are consistent with at least one Mn−Mn interaction at 3.3 Å per PS II (vide infra for Ca contribution).

Most Mn model compounds of nuclearity >2 contain Mn−Mn distances at >3 Å. In complexes that contain two μ_2-carboxylato bridges and/or one μ_2-oxo bridge, the Mn−Mn distance is greater than 3 Å, and in some complexes can be as large as 3.5 Å. By comparison with the structural motifs present in multinuclear Mn complexes we proposed that the Mn cluster in PS II consists of a pair of di-μ-oxo-bridged Mn binuclear clusters linked through a mono-μ-oxo bridge. The 2.7 Å Mn−Mn distance is characteristic of di-μ-oxo-bridged models, and the 3.3 Å Mn−Mn

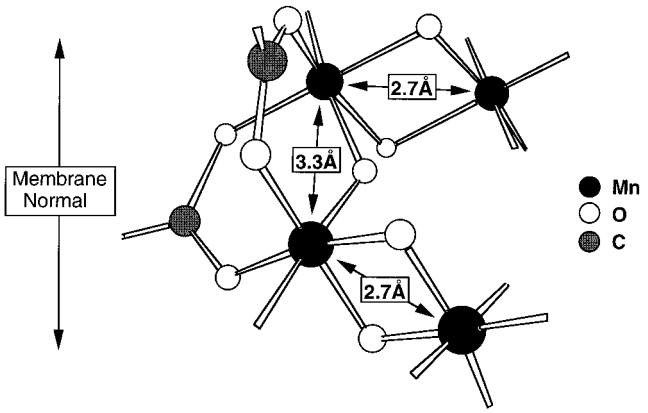

Figure 13. The proposed model for the Mn complex in the oxygen evolving complex of photosystem II. The simplest interpretation of the EXAFS data is that there are two di-μ-oxo-bridged Mn clusters which are bridged by a mono-μ-oxo-bridging ligand. The Mn−Mn distance in each of the di-μ-oxo-bridged clusters is ~2.7 Å, and the Mn−Mn distance between the Mn atoms linked by the mono-μ-oxo bridge is 3.3 Å. The relative orientation of the 2.7 and 3.3 Å vectors, with respect to the membrane normal, is derived from EXAFS dichroism data. (Reprinted from ref 6a. Copyright 1992 VCH Publishers.)

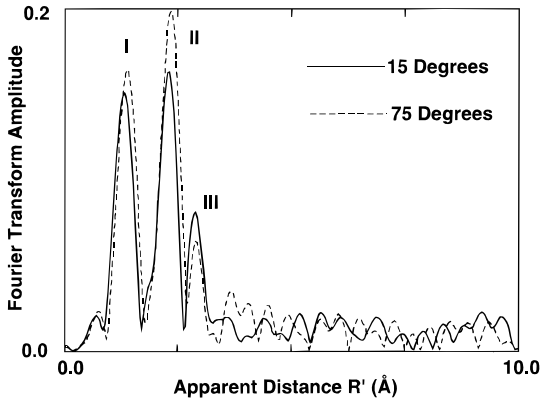

Figure 14. Fourier transforms of the k^3-weighted Mn EXAFS data (3.5−11.5 Å^{-1}) of oriented PS II membranes in the S_1 state from spinach. The solid line and dashed line are data from an oriented sample when the membrane normal is oriented 15° and 75°, respectively to the polarization direction of the X-rays. (Reprinted from ref 47b. Copyright 1994 American Chemical Society.)

distance is characteristic of mono-μ-oxo-bridged Mn−Mn distances. The dimer-of-dimers model (Figure 13) was proposed on the basis of the above data.[46c]

From polarized EXAFS the orientation of the OEC within the membrane has been determined, and the relative placement of the 2.7 and 3.3 Å vectors in the proposed model in Figure 13 is based on the orientation data. Cramer and co-workers[47a] were the first to determine the dichroism of the 2.7 and 3.3 Å Mn−Mn vectors using oriented chloroplasts. Subsequently, the dichroism has been determined using oriented PS II particles in the S_1 and S_2 states.[47b] The Fourier peaks exhibit significant orientation dependence, as shown in Figure 14. The two 2.7 Å vectors, which are characteristic of di-μ-oxo-bridged Mn atoms, are oriented at an average angle of 60° with respect to the membrane normal. The 3.3 Å vector that connects the two "dimers" makes an average angle of 43° with respect to the membrane normal (see below for a refinement of these angles).

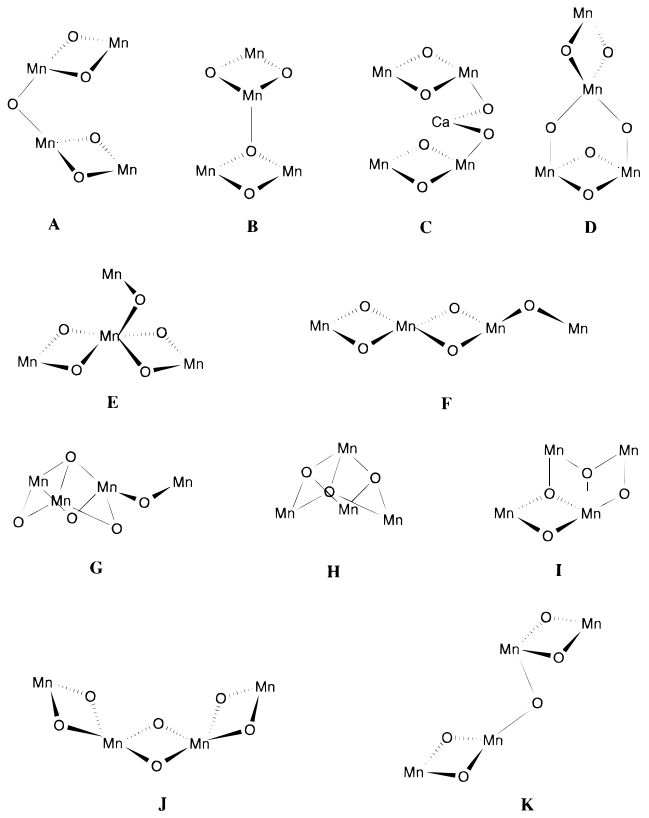

Figure 15. Arrangements of four Mn and associated bridging atoms giving Mn−Mn distances of 2.7 and >3 Å. The relation of these structures to existing tetranuclear Mn models is described in the text. The predicted coordination numbers for the neighboring Mn and bridging O atoms in these compounds are compared with those determined from EXAFS studies of the OEC in Table 1. (Adapted from ref 46b. Copyright 1994 American Chemical Society.)

2. Evaluation of Models for the OEC

The arrangement of Mn atoms proposed by our group is one of the simplest based on a reasonable interpretation of all of the data available. The EXAFS data of several multinuclear Mn model compounds have been analyzed and compared with the interactions in the OEC. It was shown earlier that a symmetric "cubane-like" or a "butterfly" configuration are incompatible with the number of 2.7 and 3.3 Å Mn−Mn vectors.[26b] A symmetric cubane was also ruled out on the basis of the dichroism observed in the EXAFS data.[47] A detailed analysis of various viable models and compatibility with EXAFS data has been carried out.[46b] It is useful to review the rationale for arriving at our proposed structure.[6a,46b,c] The EXAFS data for the OEC in both PSII membranes from spinach and PSII particles from *Synechococcus* sp. contain scatterers at >3 Å average distance from the Mn and are dominated by contributions from short Mn−O interactions at 1.8 Å and Mn−Mn interactions at 2.7 Å. There are many possible ways to arrange four Mn that include Mn−Mn distances of both 2.7 Å and 3.3 Å. Several types of possible structures are depicted in Figure 15. These are grouped roughly into "dimer-of-dimers" (A−D, K), "trimer-monomer" (E−G), and "tetranuclear" (H−J) clusters. With the exception of J, each of these structures contains a combination of

Table 1. Estimated Numbers of Scatterers per Mn Atom for Selected Multinuclear Mn Structures Shown in Figure 15

model	Mn−O at 1.8 Å (OEC 2−2.5)	Mn−Mn at 2.7 Å (OEC 1−1.5)	Mn−Mn at 3.3 Å (OEC 0.5−1)
A	2.5	1	0.5
B	2.25	1	1
C	2.5	1	1
D	3	1	1
E	2.5	1	0.5
F	2.5	1	0.5
G	2.75	1.5	0.5
H	2.25	1.5	1.5
I	2.5	1.5	1
J	3	1.5	–
K	2.5	1	0.5

∼2.7 and ∼3.3 Å Mn−Mn vectors. Mn−Mn vectors of 2.7 Å are expected for structures bridged by two oxo species, and vectors of ∼3.3 Å are expected for structures connected by a single oxo bridge. In Table 1 and Figure 15 both μ_2-oxo and μ_3-oxo bridges are approximated as having Mn−O distances of ∼1.8 Å [all structures are assumed to be Mn(III) or Mn(IV), and not to contain Mn(II)], and carboxylato bridges are not included.

With the exception of J,[48b] none of the structures in Figure 15 has yet been synthesized as a high-valent Mn compound. There are several similarities to existing inorganic models. A symmetric "dimer-of-dimers" model similar to A and C has been characterized, with ∼4 Å distance between the di-μ-oxo-bridged binuclear units.[48c] Model E is found as part of a higher nuclearity cluster,[48d] and model I has been synthesized as $Mn_4(II_2,III_2)$.[48e] The tetranuclear cluster H is closely approximated by the Cl-bridged distorted cubane.[48f] Cluster D was recently pictured in a theoretical study,[48g] and C was also recently proposed.[48h]

For each of the structures shown in Figure 15, the expected number of scatterers (per Mn) for the bridge (O at ∼1.8 Å), short metal (Mn at ∼2.7 Å), and long metal (Mn at ∼3.3 Å) interactions are listed in Table 1. Table 1 also includes the parameters for the OEC that are predicted from our EXAFS studies. The number of Mn−O scatterers in complexes D and J is somewhat higher than predicted from the OEC EXAFS. Protonation of a single bridge, however, could lengthen two Mn−O distances to the ≥1.9 Å distances included in the disordered terminal-ligand shell for the OEC. The number of 1.5 Mn−Mn scatterers at 3.3 Å in complex H, the distorted cubane or pyramidal complex, is also higher than expected for the OEC. As discussed above, the determination of the number of scatterers at this distance in tetranuclear Mn complexes can be difficult. However, the longer distance scatterers in the EXAFS of the OEC resemble the simple binuclear complexes both qualitatively and in fitting analysis behavior. This comparison favors Mn−Mn scatterers at ∼3.3 Å as found in complexes A, E, F, and G. Complex A (or K) is the simplest combination of distances and coordination numbers that fits the OEC EXAFS data and is also compatible with EPR and orientation-dependent EXAFS studies on PSII membrane preparations. For these reasons we have proposed A as a working model for the structure of the Mn complex in the OEC.

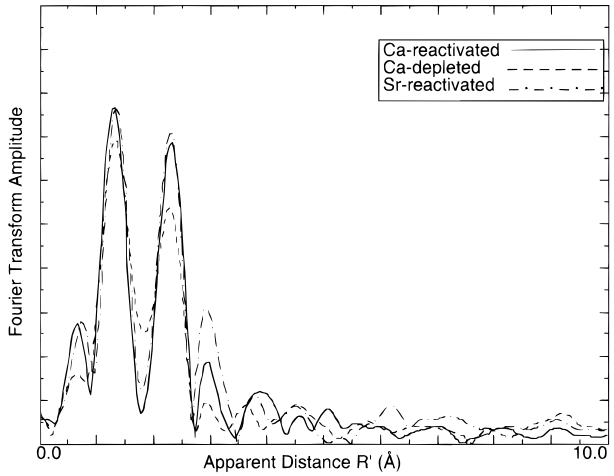

Figure 16. Fourier transform power spectra of Mn EXAFS *k*-space data for Ca- and Sr-reactivated PS II (solid line, long dashes, respectively), and Ca-depleted PS II (short dashes). The spectra are clearly different in the amplitude of the peak at ∼3 Å, which is enhanced in the Sr-reactivated sample and decreased in the Ca-depleted one.[52b]

C. The Structural Role of the Cofactors Ca and Halide

1. Proximity of Ca to Mn

Ca is a cofactor essential for oxygen evolution.[4] There are several lines of evidence that suggest a close proximity between the essential Ca and the Mn cluster. Mn depletion has a significant effect on the binding constants of Ca to the Mn-OEC.[49] It has been shown that Sr can replace Ca with partial restoration of oxygen evolution.[50a] The proximity of Sr to the Mn cluster is implicit from the fact that the multiline EPR signal of Sr-reconstituted membranes is modified relative to that of control samples.[50b]

Analysis of X-ray edge spectra reveals no significant differences in oxidation state or symmetry between Ca- and Sr-reactivated preparations. In the EXAFS data from Latimer et al.[52a,b] the amplitude of the Fourier transform peak due to scatterers at distances >3 Å is larger for samples reactivated with Sr relative to that for Ca-reactivated samples (Figure 16). The calculated parameters favor a model where both Mn and Ca (or Sr) scatterers contribute to the Fourier peak at >3 Å. Other models for the ∼3 Å peak with multiple Mn−Mn interactions or multiple Mn−Ca(Sr) interactions can also be fit to the data, but are considered less likely. A Ca-binding site at this distance from a metal cluster represents an unusually close association for a biological system and may indicate an intimate role for Ca in water oxidation. The XAS studies of Penner-Hahn et al. with Ca or Sr, or Dy which inhibits O_2 evolution, do not show significant improvement in their fits to Mn at 3.3 Å by including Ca, Sr, or Dy, in the respective samples.[53a,b] The third Fourier peak is best fit by MacLachlan et al. by Ca at 3.7 Å to Mn.[46a] It is important to point out that different preparations

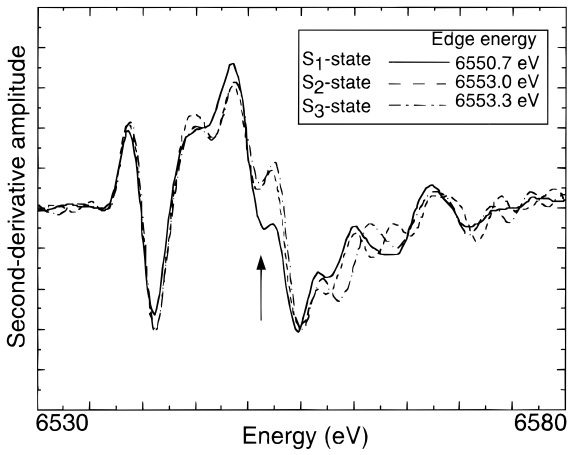

Figure 17. Second-derivative Mn K-edge spectra from calcium-depleted PS II preparations in the S_1 (solid line), S_2 (short dashes), and S_3 state (long dashes). Second-derivative spectra are presented to emphasize the shape of the edges. The rising part of the edge (6545−6555 eV) is most indicative of oxidation state changes, and clear differences can be seen between the S_1 and the S_2 or S_3 spectra at about 6550 eV (see arrow). In this region, the S_2 and S_3 edges are very similar in shape, while the S_1 edge is clearly lower in energy (see inset). Edge inflection point energies (inset) were taken from the zero crossing in the second derivative spectrum (see arrow). The S_2 and S_3 states were generated by illumination of calcium-depleted preparations in the S_1 state at 0°C for 1 min. S_2 samples contained DCMU to prevent more than one turnover.[52b]

and methods of XAS analysis were used by the different groups and could have contributed to the variation in the interpretations. However, at this time the reason for the differences in the data and/or interpretations is unresolved.

Depletion of Ca^{2+} by NaCl wash in the presence of EGTA or by a low pH citrate treatment results in a dark-stable multiline EPR signal, which is different from EPR spectra obtained with either the Ca^{2+}- or Sr^{2+}-containing preparations.[18a] It has been shown, that besides Ca depletion, the presence of EGTA or citrate is required for the EPR signal from the S_2 state to be modified and stabilized,[51a] and that the modification of the S_2 state may be because of the binding of the chelator to the Mn complex.[51b,c] It has also been shown that Ca-depleted samples do not advance beyond the S_3 state and that this S_3 state is characterized by a broad EPR signal at $g = 2$.[18a,b] We have collected Mn K-edge and EXAFS data from Ca-depleted samples prepared using a low pH treatment in the S_1, S_2, and S_3 states.[52b] Ca depletion has a marked effect on the Mn K-edge spectra and EXAFS, especially in the S_1 state, which provides a clear indication that removal of Ca^{2+} and the presence of citrate perturbs the structure of the Mn complex. Similar Mn K-edge spectra for the S_1 state have been reported by Ono et al.[52c] Analysis of the S_2 and S_3 states shows that there is essentially no change in the Mn K-edge position or shape between these two states (Figure 17). This provides direct evidence that Mn is not oxidized during the S_2 to S_3 transition in Ca-depleted preparations and that the oxidizing equivalent is indeed stored elsewhere, probably on an amino acid residue as suggested by EPR studies and confirmed recently to be tyrosine Y_Z.[20]

2. Is Chloride a Ligand of Mn?

Cl^- is an essential cofactor for O_2 evolution.[4] Cl^- can be replaced by Br^- with full retention of activity. F^- inhibits O_2 evolution;[4] however, a recent report indicates that F^- partially activates O_2 evolution compared to Cl^--depleted samples.[54a] Studies by Rashid and Homann[54b] have shown that I^- also partially reactivates O_2 evolution. The requirement for a halide ion has led some workers to postulate that the halide ion is a ligand to one or more of the Mn atoms in the complex, while other workers favor a model where the halide is required to stabilize a positive charge near the Mn complex. On the basis of a study using $^{36}Cl^-$ Andréasson and Lindberg[55] have proposed that halide may not be essential for oxygen evolution; recently, the data has been reinterpreted by van Vliet and Rutherford[54a] to reach the conclusion that one Cl^-/PS II is essential for O_2 evolution.

Our earlier work showed that Cl^- or Br^- is required to generate the MLS which is characteristic of the S_2 state. High-resolution EPR studies of Cl^- or Br^- containing samples from spinach,[37a] and from PS II preparations from *Synechococcus* grown in either Cl^- or Br^- media, also do not exhibit any differences.[26e] When Cl^- is substituted by F^-, no multiline signal is seen in the S_2 state. There is a signal at $g = 4.1$.[16a] It is possible, however, that the magnetic hyperfine interactions of a halide ligand may be too small to be detectable by conventional EPR methods. ESEEM studies have been inconclusive to date in identifying any hyperfine interactions from the halide ion. Recent ESEEM studies, while presumably showing differences between Cl^-- and Br^--containing samples, could not distinguish whether the differences in electron spin-echo modulations arose from ligand atom interaction or from Cl or Br in the buffers.[57] It has been shown that PS II particles which have been depleted of Cl^- do not have an EPR multiline signal in the S_2 state.[37a] There is an EPR signal at $g = 4.1$, that is not sensitive to Cl^- depletion.[56a] However, in this case the OEC can no longer advance to higher S states. It was found that the S_2 state can be formed in the absence of Cl^-, and subsequent addition of Cl^- after illumination results in an EPR multiline signal.[56a] XANES studies of Cl^--depleted PS II samples subjected to flash illumination confirm that Mn is oxidized after one flash.[56b] These studies indicate that the Mn−OEC can be oxidized from the S_1 to the S_2 state in the absence of Cl^-, but that Cl^- is required to generate the multiline EPR signal.

XAS methods have also been inconclusive in determining the presence of the halide in the ligation sphere of Mn.[26b,c,28b,46a,b,47a] The perturbation of the Mn−Mn distance by F^- is the most direct evidence available of halide binding. XAS studies of F^--inhibited samples show that one of the two 2.7 Å distances is increased to about 2.8 Å which is suggestive of F^- binding to the Mn cluster.[58a] XAS data from Br^- grown *Synechococcus* are, however, consistent with one halide being in the first coordination sphere of Mn, but the evidence is not conclusive.[26e] Also, in studies of oriented native PS II, George et al. found that they could not rule out the presence of one Cl^- per four Mn, but the spectral contributions

were minimal and the results were not conclusive.[47a]

Suffice it to say that the binding of Cl^- to Mn has been a matter of controversy and that there is considerable interest in the field to gain definitive physical evidence for or against halide ligation to Mn.

D. Ligands of Mn

The Mn complex can have a total of 24 ligands if each of the 4 Mn atoms is octahedrally coordinated. The Mn K-edge energies and EXAFS data support mostly O or N ligand atoms. In the dimer-of-dimers model 10 such positions are accounted for by the oxo-bridges, and four more ligand sites by two carboxylate bridges. More carboxylate bridges could be present within the constraints of the Mn−Mn distances observed for the OEC. Glutamate and aspartate residues in the D1 and D2 polypeptides are likely candidates for providing these ligands. Terminal carboxylate ligand atoms are most likely provided by amino acid residues either in a monodentate or bidentate form, histidine residues, the cofactor halide, and other N- or O-containing residues.[2a] It is possible that there exist some exogenous N- or O-containing ligands, although there is no evidence for or against such ligands. The best evidence for putative ligands has come from site-specific mutagenesis studies. The mutagenesis of residues that alter growth patterns and oxygen evolution includes the carboxy terminus of the D1 polypeptide[59] and several Asp, Glu, and His residues on D1 and one Glu residue on D2. The reader is referred to recent reviews in this field for details (ref 2a and references therein).

FTIR spectroscopic studies using isotopically labeled PS II preparations implicate a carboxylate residue in Mn ligation.[60] Early ESEEM studies using ^{14}N- or ^{15}N-labeled PS II preparations from *Synechococcus* sp. provided evidence for N ligation, probably from a His residue to Mn.[61a] Recently, this has been confirmed by ESEEM using PS II preparations from *Synechocystis* 6803 wherein all histidines were labeled with ^{15}N.[61b]

NH_3 and F^-, both inhibitors of O_2 evolution, are also potential ligands of Mn. The modification of the MLS spectra upon addition of NH_3[62a] and ESEEM studies using $^{14}NH_3$ or $^{15}NH_3$ demonstrated that NH_3 becomes a ligand of Mn.[62b] EXAFS studies showed that the Mn−Mn distance increases in NH_3-treated PS II and proposed that an oxo-bridge is replaced by an amido bridge (see below for details). EXAFS studies also showed that F^--treated PS II perturb the Mn−Mn distances; this has been rationalized on the basis of F^- ligation to Mn (vide infra).

V. Structural Changes During S-State Transitions

A. S_1 to S_2 State (Multiline EPR) Advance

Detailed evaluation of Mn EXAFS data collected at 10 K on the OEC from PS II has been carried out on preparations from both spinach and the cyanobacterium *Synechococcus* sp. poised in the S_1 or the S_2 state; the latter state was characterized by the multiline EPR signal (S_2 MLS). The overall structure is almost invariant in this S_1 to S_2 transition (Figure 18). However, subtle but reproducible changes are found in the relative amplitudes of the Fourier transform peaks due to the bridging and terminal ligand atoms O, N (1.8−2 Å) and Mn (∼2.7 Å) neighbors upon cryogenic advance from the S_1 to the S_2 state.[26e,46b] The Mn−ligand and Mn−Mn distances change in a manner which is consistent with a change from a III,III di-μ-oxo-bridged binuclear moiety to the corresponding III,IV moiety.

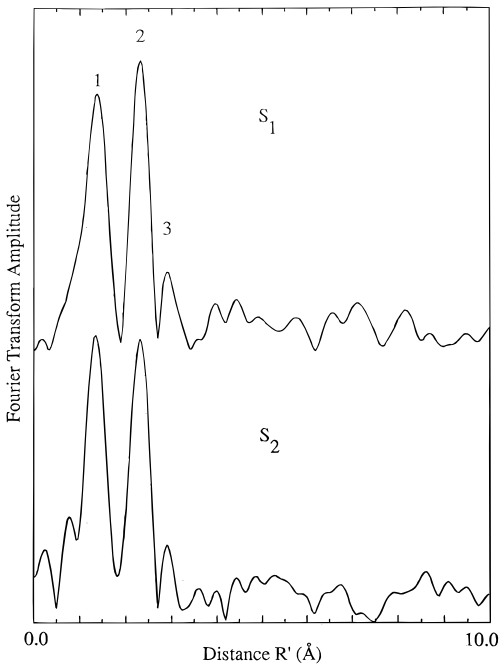

Figure 18. Fourier transforms of k^3-EXAFS data (3.5−12.0 $Å^{-1}$) from *Synechococcus* samples in the S_1 and S_2 states. The Fourier transforms are similar to those shown above. Note the similarity of the Fourier transforms in the S_1 and S_2 states.

Polarized EXAFS studies on oriented PS II in S_1 and S_2 states show that there is heterogeneity in the 2.7 Å vectors, which is suggestive that the two binuclear species are not completely equivalent in the S_1 and S_2 (multiline EPR) states.[47b] In the S_1 state the best fit for the second Fourier peak is at 2.74 Å when the measurements are done with the membrane normal at an angle of 75° to the X-ray **e** vector, while the best fit is at 2.71 Å when the membrane normal is at 15° to the X-ray **e** vector. Fitting the angle dependence of the amplitude of the 2.7 Å vector leads to 1.1 ± 0.1 Mn−Mn interactions at an average angle of 60 ± 7°, with respect to the membrane normal. The number of Mn−Mn interactions implies at least two 2.7 Å vectors for the OEC; thus the angle of 60° represents an average value. Interestingly, advancing to the S_2 state leads to a shortening of the 2.74 Å distance to 2.71 Å, when the membrane normal was at 75° to the X-ray **e** vector, with no change in the distance of 2.71 Å at the angle of 15°. This leads to the proposal that a Mn atom associated with the vector having the greater angle to the membrane normal undergoes oxidation. We propose that the asymmetry of the S_1 state can be resolved into a shorter Mn(IV)−Mn(IV) 2.71 Å vector which forms an angle less than 60° to the membrane normal, and a longer Mn(III)−Mn(III) 2.74 Å vector which makes a greater than 60° angle with the

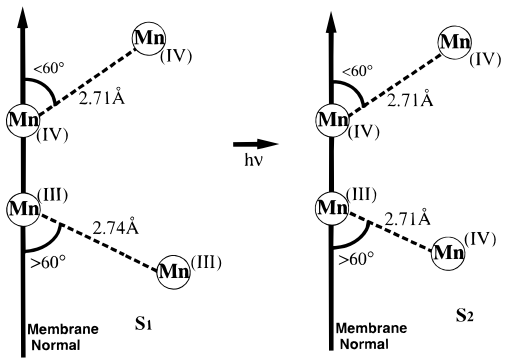

Figure 19. Proposed model for the change in Mn−Mn distance for the vector that is oriented at greater than 60° to the membrane normal, upon the S_1 to S_2 transition. (Reprinted from ref 47b. Copyright 1994 American Chemical Society.)

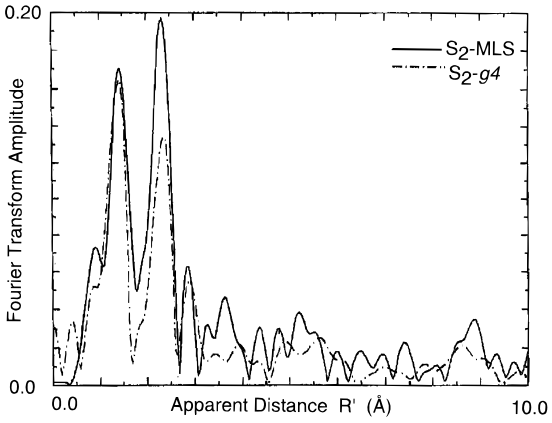

Figure 20. Fourier transform spectra of the k^3-weighted Mn EXAFS of the S_2−g4 sample (dash−dot) and the S_2-multiline sample (solid). The significantly smaller second peak in the EXAFS of the S_2−g4 sample indicates a more disordered system. The decrease of the third peak amplitude is less than that of the second peak. (Reprinted from ref 63. Copyright 1994 American Chemical Society.)

membrane normal. We speculate that the Mn(III)−Mn(III) dimer associated with this longer vector is oxidized to Mn(III)−Mn(IV) on the S_1 to S_2 transition (Figure 19).

B. S_1 to S_2 State ($g = 4.1$ EPR) Advance

Mn XAS spectra have been collected from PS II samples from spinach in the S_2 state produced by illumination at 130 K and characterized by the $g = 4.1$ EPR signal. The Mn K-edge spectra show not only a shift to higher energy, indicating oxidation of Mn, but also a second derivative with a shape different from that of the S_2 state with the multiline EPR signal.[63] The EXAFS results are quite surprising (Figure 20); while there are only subtle changes observed in samples in the S_2 state produced by illumination at 190 K (characterized by the MLS) compared to samples in the S_1 state, the samples produced in the S_2 state by illumination at 130 K ($g = 4.1$ EPR signal) show significant differences in the magnitude of the second Fourier peak at ~2.7 Å. This peak is best fit by two different Mn−Mn distances of 2.73 and 2.85 Å.[63] The data again have been interpreted as evidence for the presence of two nonequivalent di-μ-oxo-bridged binuclear structures in the Mn

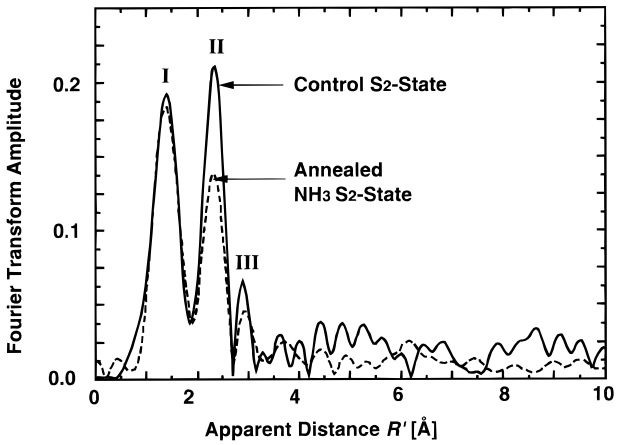

Figure 21. Fourier transforms of the k^3-weighted Mn EXAFS of untreated PS II samples (solid line) and annealed, ammonia-treated PS II samples. Both samples were poised at the S_2 state by illumination at 195 K, after which the ammonia-treated sample was annealed at 4 °C. (Reprinted from ref 64. Copyright 1995 American Chemical Society.)

cluster of the S_2 $g = 4.1$ state. This heterogeneity is not present in samples that were annealed to 190 K, a protocol which results in the disappearance of the $g = 4.1$ EPR signal and the appearance of the MLS signal. Clearly a small structural rearrangement seems to occur on illumination at 130 K concurrent with the production of the $g = 4.1$ EPR S_2 state. We speculate that this perturbation modulates the magnetic coupling between the two binuclear moieties resulting in either a $g = 4.1$ or multiline EPR signal (see next section). Recently, a series of oxo-bridged Mn complexes have been isolated in three different protonation states of the bridges without a change in the other ligands or the oxidation state of the Mn.[29] It is interesting that each successive protonation resulted in a lengthening of the Mn−Mn distance from 2.7 to 2.8 to 2.9 Å. There was also a concomitant decrease in the antiferromagnetic coupling without a significant change in the Mn K-edge absorption energies. Pecoraro and co-workers[29] speculate that the difference between the S_2 state characterized by the MLS and the $g = 4.1$ state might be a single protonation of an oxo bridge.

C. NH_3- or F^--Modified S_2 State

Recently, the effect of NH_3 on the 2.7 Å vectors has been investigated. NH_3, an analog of the substrate water, inhibits oxygen evolution and produces a $g = 4.1$ EPR signal on illumination at 195 K; annealing to 273 K then produces an altered MLS. Earlier ESEEM studies using $^{14}NH_3$ or $^{15}NH_3$ showed that NH_3 is directly coordinated to Mn. XAS studies show that one of the 2.7 Å vectors is perturbed in NH_3-treated samples, with the distance increasing to 2.85 Å, providing further evidence for the presence of two dissimilar di-μ-oxo-bridged moieties (Figure 21).[64]

The orientation of the vectors with respect to the membrane plane has been determined by using oriented multilayers of PS II treated with NH_3. Figure 22a shows polar plots of the angle dependence of two vectors, from which one can derive the angle at which the vectors are present in the membrane (Figure 22b). The 2.7 Å vector which is at an average

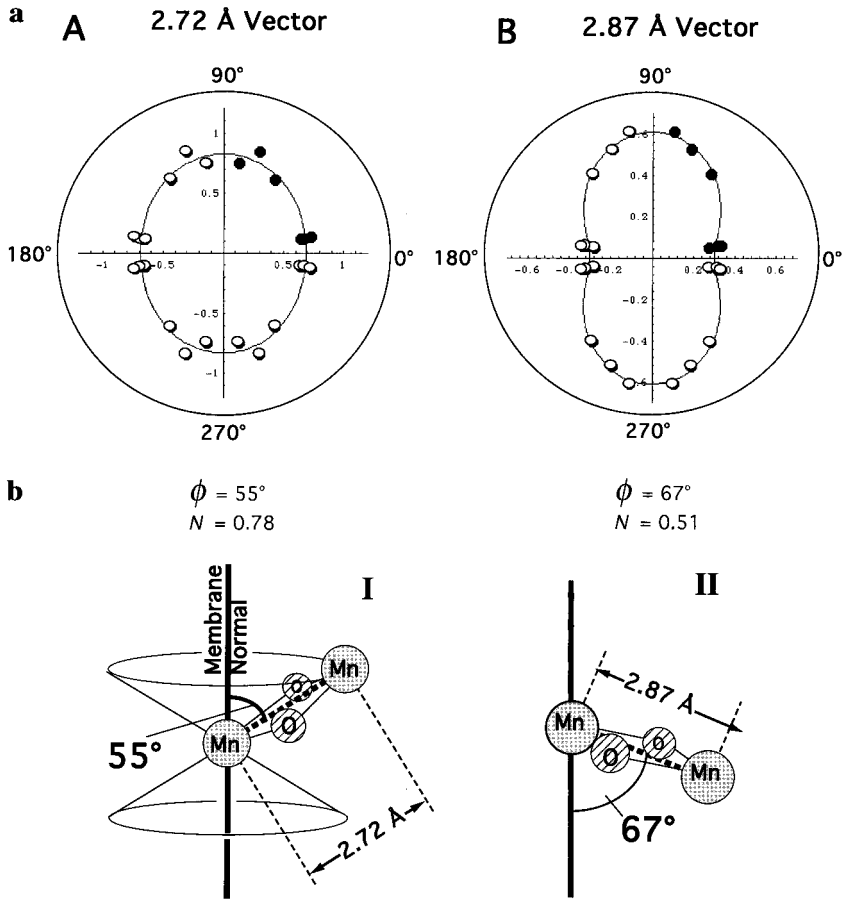

Figure 22. (a). Angle dependence of the apparent coordination numbers. The apparent coordination numbers $N(\theta)$ are plotted versus the detection angle, in the form of a polar diagram. The solid line has been obtained by fitting the experimental data to a known equation using a least-square error criterion. Solid points are data from five oriented samples and one unoriented sample. The open dots are data points which have been mirrored for clarity. The error ranges were determined as the parameter values for which the sum of residuals increased by 100%. The resulting average angles with respect to the membrane normal and isotropic coordination numbers are shown. (b) Building blocks for a structural model of the PS II manganese complex. The Mn−Mn distances and the angles with respect to the membrane normal were determined for the NH_3-treated Mn complex. The relative orientations of the individual Mn binuclear clusters are not uniquely determined by the experimental results; each angle corresponds to a double cone of possible orientations as indicated in part a of this figure. (Reprinted from ref 64. Copyright 1995 American Chemical Society.)

angle of 60° to the membrane normal in native samples (see above) can now be resolved into two angles. The 2.73 Å vector is oriented at an angle of 55° and the 2.87 Å vector is at 67° (Figure 23). The structural heterogeneity may have implications for the mechanism of water oxidation.

It has been shown that treatment with F^-, which inhibits oxygen evolution and generates a $g = 4.1$ EPR signal, also leads to heterogeneity in the 2.7 Å vectors (see above).[58a] On the basis of these studies an alternative proposal for the $g = 4$ form of the S_2 state, from those discussed in the previous section, has been considered by DeRose et al.[58a] In this model (Figure 24), the Mn atoms in the OEC are in redox equilibrium such that oxidation of one particular Mn results in the $g = 4$ form of the enzyme, but migration of the oxidizing equivalent to a different Mn (for example, on annealing) results in the multiline EPR signal. This idea has been previously suggested on the basis of theoretical calculations of the effects of exchange coupling within a Mn tetramer.[58b] Within the structural model of a pair of binuclear Mn complexes [A,B], this model can be interpreted in terms of the oxidation of one binuclear complex giving rise to the $g = 4$ signal [form A_{ox}, B] but oxidation of the other complex resulting in the multiline signal [form A, B_{ox}]. The configuration [A_{ox}, B] is also proposed to be generated on treatment with F^-; a treatment that produces the $g = 4.1$ EPR signal, and heterogeneity in the Mn−Mn distance. This proposal gains credence in light of the recent experiments that have correlated the $g = 4.1$ EPR signal in native samples to the absorption in the near-infrared at 820 nm after the generation of an S_2 state by illumination with actinic light.[35] The transition caused by the absorption at 820 nm has been assigned to an intervalence charge transfer from Mn(III) to Mn(IV).

D. S_0 State

Guiles et al.[30b] prepared samples in an S_0-like state by illuminating S_1-state samples that had been exposed briefly to a solution of 40 μM hydroxyamine. Such samples exhibited an edge shift to an energy lower than that of the S_1 state. The EXAFS data of these S_0-like or S_0* samples were very different from those of the other three states, showing a marked decrease in the amplitude of the peaks in the Fourier transform. Detailed EXAFS analysis showed that there is a larger spread of Mn−Mn and Mn−ligand distances in the S_0* state compared to that in the S_1

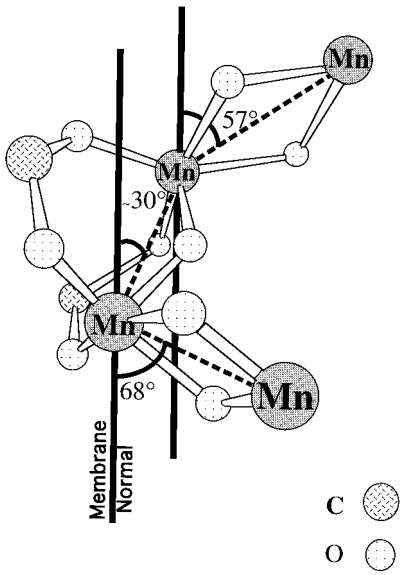

Figure 23. The proposed orientation of the Mn complex with respect to the membrane normal. By rotation of the structure proposed by Yachandra et al.[46c] about the membrane normal, the set of angles indicated in the figure is obtained. The rotation was done in such a way as to obtain angles for the 2−7 Å Mn−Mn distances close to the experimentally determined values of 55° and 67°, respectively. (Reprinted from ref 64. Copyright 1995 American Chemical Society.)

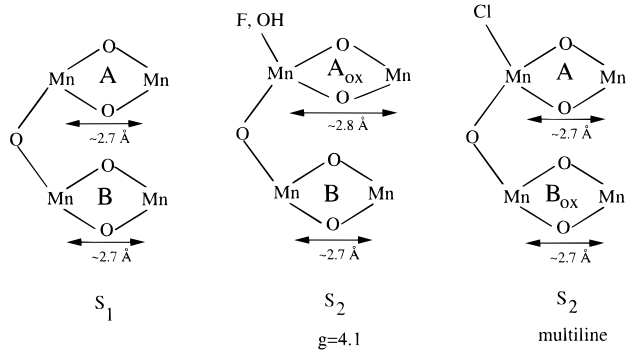

Figure 24. Structural model for the $g = 4$ form of the OEC. In this model, the OEC is arranged as a pair of binuclear centers [A, B], connected by a mono-μ-oxo bridge, which are exchange coupled to produce the EPR signals found in the S_2 state. Oxidation of center A by either low-temperature illumination or illumination of F^--inhibited samples results in a longer Mn−Mn distance in A_{ox} and a ferromagnetically coupled cluster that gives the $S = {}^5/_2$, $g = 4$ form of the enzyme. In untreated samples, illumination at 190 K or "annealing" of samples illuminated at a lower temperature results in rearrangement to form B_{ox}, which is constrained to smaller changes in the Mn−Mn distance upon oxidation, compared to form A. (Reprinted from ref 58a. Copyright 1995 Elsevier.)

state. The best fit for the second Fourier peak was obtained with two Mn−Mn distances at 2.69 and 2.87 Å, indicating that one of the oxo-bridged structures might be different from that in the S_1 state. The analyses were consistent with the presence of a significant quantity of Mn(II). The bond lengths between Mn(II) atoms and their ligands are typically 0.1 to 0.2 Å longer than those of Mn(III) and Mn(IV). The resulting phase difference between the backscattered waves from the low- and high-valent Mn atoms leads to destructive interference and hence to a diminished amplitude of the EXAFS and the

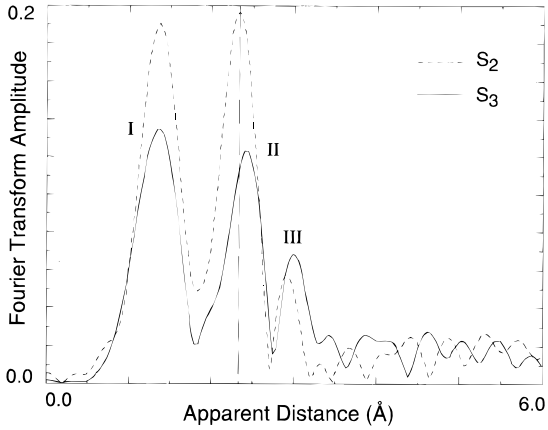

Figure 25. Fourier transforms of the k^3-weighted EXAFS data (3.5−11.5 $Å^{-1}$) of PS II-enriched membranes in pure S_2 and S_3 states. The vertical line designates the maximum of peak II of the S_2 transform, and it is clear that peak II is shifted to a longer distance for the S_3 state. Preliminary fitting to peak II confirms a lengthening of Mn−Mn interactions. (Reprinted from ref 65. Copyright 1995 Kluwer Academic Publishers.)

Fourier transform features. The edge data were suggestive of the presence of Mn(II), and the EXAFS provided additional information supporting the presence of Mn(II) in the S_0 state.

E. S_2 to S_3 State Transition

Earlier XAS data from the S_3-state samples produced by a cryogenic double turnover method indicated increased disorder in the peak at 2.7 Å, indicative of the presence of two nonequivalent di-μ-oxo-bridged clusters in the S_3 state.[30a] The principal result of that work was that a small but significant structural change was found to accompany the S_2−S_3 transition. Specifically, the second Fourier peak, representing Mn scatterers at about 2.7 Å, was better simulated by two slightly different distances differing by 0.15 Å. Such a change in distance was somewhat surprising in view of the fact that, because of the absence of an edge shift, no oxidation of Mn appeared to have occurred. Nonetheless, it was the first indication that the cluster contained two different di-μ-oxo bridged distances. This provided the first indication that there might be two nonequivalent binuclear species.

The first EXAFS results for S_3-state samples created under physiological conditions with saturating flashes were recently reported.[65] Pure S_3 EXAFS spectra were generated from linear combinations of the flash-induced EXAFS spectra, with each coefficient obtained from the best fit of the flash-induced multiline EPR signal (MLS) oscillation pattern to Kok's model. The Fourier transform of a S_3 sample is shown in Figure 25. The preliminary data show that the second Fourier peak is shifted to a longer distance compared to that in the S_2 state. The peak can be best fit to two Mn−Mn interactions at a distance of ~2.8 Å, or to one Mn−Mn interaction at ~2.8 Å and the other at ~3.0 Å. These results contrast with the fit for the S_2 (or the S_1) state where one obtains two Mn−Mn interactions at ~2.7 Å. It is interesting to note that the structural perturbation involved in the S_3 state is also different from the

perturbation observed in the S_2 states for ammonia-treated samples, fluoride-treated samples, or untreated samples illuminated at 130 K ($g = 4.1$ EPR signal). Each of these altered S_2 states gives a two-shell Mn−Mn fit of around 2.71 and 2.85 Å that is consistent with the alteration of one of the two di-μ-oxo-bridged Mn binuclear units proposed in our model. Preliminary fits for the S_3 data, however, show an elongation of both bridges. Although each of the three altered S_2 states may have very similar structures, the S_3 state's structure is distinctly different.

Either of the fit results represents a significant structural change in the complex. Protonation of the $Mn_2(\mu\text{-oxo})_2$ bridge, in the S_3 state prior to peroxide formation, as proposed by Pecoraro et al.,[9e,f,66] would result in such an increase in the Mn−Mn distance. It has been suggested by Renger[67] that a peroxo-bridged Mn structure is likely for the S_3 state, while other workers suggest that a peroxo bridge cannot form at the S_3 state.[68] The Mn−Mn distance in peroxo-bridged complexes is likely to be greater than 3 Å, assuming that the peroxo group replaces one of the di-μ-oxo bridges. Replacement of two of the μ-oxo bridges by a peroxo bridge during the S_2 to S_3 transition implies a simultaneous reduction of Mn; such a reduction is not supported by the Mn K-edge spectra of the S_2 and S_3 states. On the other hand, if the bridge is formed between the two proposed di-μ-oxo-bridged structures, it will show up as a change in the Fourier peak at 3.3 Å which we observe in both the S_1 and S_2 states. Our preliminary data for the S_3 state show that the third Fourier peak is at a longer distance, about 3.4 Å, compared to the 3.3 Å distance observed in the S_1 and S_2 states. It is interesting to note in this context that in a binuclear complex where the Mn atoms are linked by a di-μ-oxo and a μ-peroxo bridge, the Mn−Mn distance "decreases" from 2.7 to 2.53 Å and the four-membered Mn_2O_2 ring is puckered.[69a] Synthesis and crystallographic characterization of a complex containing a trinuclear μ_3-oxo-bridged Mn_3(III) with a bound μ-peroxo group has been reported. The Mn atoms linked by one μ_3-oxo and a peroxo-bridge are at a distance of 3.14 Å.[69b] A side-on peroxo-bound mononuclear complex has been synthesized recently, but there are no multinuclear complexes with only a peroxo bridge between the metal atoms.[69c] An alternative and very likely explanation for the changes seen in the Mn−Mn distances during the S_2 to S_3 transition arises from the results with binuclear Fe complexes (see below), where the oxidative equivalent is proposed to be delocalized on the $Fe_2(\mu\text{-oxo})_2$-bridged unit.

VI. Mechanism of Water Oxidation and O_2 Evolution

The kinetic data from photosynthetic oxygen evolution have provided the basis for the S-state intermediates proposed by Kok that form the catalytic cycle.[3a] It is known that there are four stable S-state intermediates, S_0−S_3, and one state, S_4, which spontaneously releases O_2 and returns to the least oxidized state, S_0. The rate-limiting step is the advance from S_3 to (S_4) to S_0 and O_2. This mechanism has had an enormous influence on thinking related to the understanding of photosynthetic water oxidation. Although it did not specify particular chemical intermediates or the stage where water molecules were taken up, the mechanism does provide a rationale for most of the experiments that measured the pattern of O_2 release.[3b] In studies of the role of Mn in this process workers have generally adopted the Kok model and have attempted to characterize the oxidation state and structural parameters of the individual S states.

The thermodynamics of the water oxidation as described by Krishtalik[70a] and modified by Brudvig and de Paula[70b] require the production of O_2 from fully deprotonated H_2O, O^{2-} (oxide). Binding of protons released from H_2O by protein residues is thermodynamically favored. Water oxidation mechanisms involving single-electron steps are deemed impossible, while two- and four-electron concerted reactions are favored.[70a] Deprotonation of H_2O to O^{2-} coupled to simultaneous protonation of nearby groups is considered the path of least resistance.[70a]

At present the step at which water binds to Mn is not known. A subtle broadening of the MLS was detected after an incubation of PS II in $H_2{}^{17}O$ in light, and this was taken as evidence that water is incorporated into the Mn site by the S_2 state.[71] ESEEM studies on the MLS of ^2H_2O-exchanged PS II showed modulations characteristic of deuterons.[72] These results provide evidence for nearby exchangeable proton sites, but it is not clear whether the protons on H_2O or hydroxo ligands to Mn generate such modulations. There was no discernible change in the width of the substructure seen on each of the major MLS lines or on the overall width of the measured CW EPR lines with ^2H_2O-exchanged PS II samples.[37a] It might be that O atoms from water are in place by the S_2 state, and the deprotonation steps have already occurred (see below). Mass spectrometry measurements of O_2 evolved after mixing PS II samples with $H_2{}^{18}O$ and subsequent illumination have provided the only other information about substrate binding to Mn. In the time scale of their experiments, Radmer and Ollinger[73a,b] found that there was no nonexchangeable water bound to the Mn complex until the S_3 state and concluded that water oxidation does not occur until the S_3 state. The proposed rationale was that oxidized water would be harder to exchange. The most recent results, by Messinger et al.[73c] based on a mixing time of 30ms, compared to the 1 min used in earlier studies, support the presence of two nonequivalent exchangeable sites in the S_3 state. Two different modes of O binding are proposed to account for the two different rates of exchange; the slow exchange site being correlated to the presence of a proposed Mn=O group. Other possibilities were not discounted, including differences in oxidation states or differences in coordination environment.

Mechanisms proposed by Brudvig and Crabtree[68] and by Christou and Vincent[74] for water oxidation have provoked much discussion. However, both mechanisms invoke structural motifs that are not entirely compatible with EXAFS data. The mechanisms also propose significant structural changes in

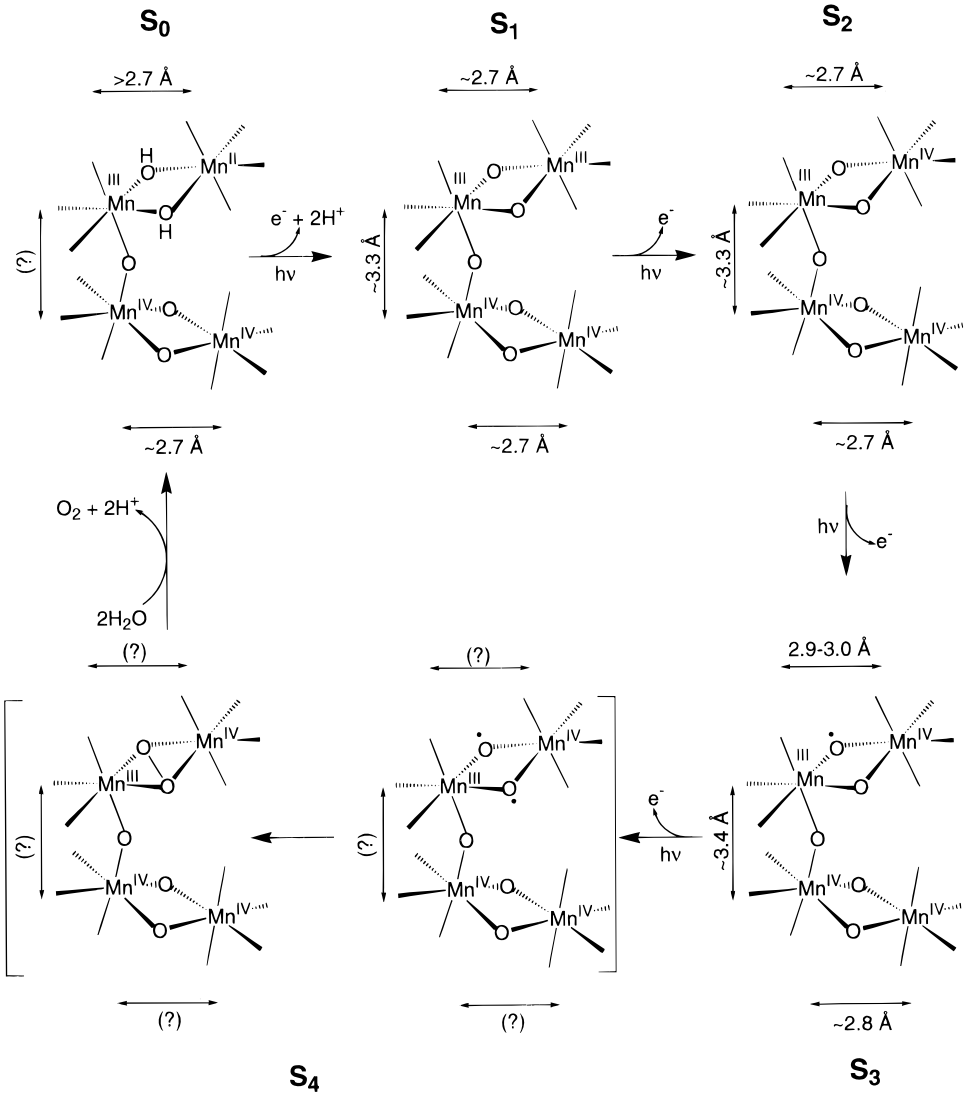

Figure 26. Mechanism proposed for water oxidation and oxygen evolution on the basis of the X-ray absorption and EPR spectroscopy data.

the Mn complex as it traverses the S-state cycle. EXAFS data do not confirm such proposed structural changes. The first proposal involves a transformation from a cubane-like to an adamantane-like structure; and the second a butterfly to cubane-like structure. Both the proposals have been important in providing a framework for exploring the mechanism, but neither is consistent with available experimental data.

Pecoraro and co-workers[9e,f,66] have proposed a detailed mechanism that involves protonation of a $Mn_2(\mu\text{-oxo})_2$ bridge at one binuclear unit in the S_3 state prior to peroxide formation. Such a mechanism could account for the increase in the Mn−Mn distance observed by EXAFS in the S_3 state and the relatively invariant structure, predominantly consisting of di-μ-oxo cores, in the S_1 and S_2 states. Successive protonation of di-μ-oxo bridges in binuclear Mn complexes has been shown to result in an increase in the Mn−Mn distance from 2.7 to 2.8 and 2.9 Å.[29]

Recently, Babcock and co-workers[75] have proposed a mechanism that involves the tyrosine Y_Z residue in each step of the S-state cycle. The crux of the proposal involves a simultaneous extraction of an electron and a proton in each of the S-state transitions, with Tyr Y_Z playing a crucial role.

We propose a mechanism for water oxidation that is based on XAS and EPR results from the S_0-S_3 states. The major criterion is the comparison of the Mn−Mn distances reported for the various S states with the structural motifs and Mn−Mn distances reported in the literature for compounds of known structure. We draw from the extensive bioinorganic chemistry of multinuclear Mn, Fe, and Cu complexes.

Figure 26 shows our proposed mechanism for photosynthetic water oxidation.

(1) The structure of the complex consists of two nonequivalent di-μ-oxo-bridged binuclear Mn clusters linked to each other by a mono-μ-oxo bridge. EXAFS provides ample evidence for the existence of two different di-μ-oxo units in the OEC. In the S_1 state the oxidation states are III_2 and IV_2 as shown by the Mn K-edge spectra. One "dimer" is proposed to be redox inert and is in the oxidation state IV,IV. The redox active binuclear center is in the oxidation state III,III. The S_1 state EPR signal has been proposed to arise from an integral spin state of $S = 1$ or 2 and is compatible with our proposed oxidation states. The oxidation states are also compatible with the alterna-

tive interpretation that the S_1 state is diamagnetic.

(2) In the transition to the S_2 state one Mn(III) is oxidized to Mn(IV). The Mn−Mn distance decreases in a manner consistent with such an oxidation. The S state characterized by the $g = 4.1$ state has a longer Mn−Mn distance either because Cl replaces one of the ligands or because one of the oxo bridges becomes protonated. The difference in exchange coupling is responsible for generating either the MLS or the $g = 4.1$ EPR signal. The Mn K-edge analysis supports oxidation of Mn and is consistent with an oxidation state of $Mn_4(III,IV_3)$ and an $S = {}^1/_2$ ground state responsible for the multiline EPR signal. An alternative explanation by DeRose et al.[58] proposed that the oxidation of one binuclear complex gave rise to the $g = 4$ signal but that the oxidation of the other complex resulted in the multiline signal (see Figure 24).

(3) The Mn K-edge inflection point data support the interpretation that Mn is not oxidized during the S_2 to S_3 transition. The increase in one of the Mn−Mn distances to 2.9 Å observed in the EXAFS data is critical for this proposal. Protonation of oxo bridge(s) could produce this increase in distance. An alternative explanation for this increase can be found in binuclear Fe chemistry (see below).

Cluster X of ribonucleotide reductase is proposed to be formally a Fe_2(III,IV) species. It has been described as a coupled system consisting of two high-spin Fe(III) plus a ligand radical;[76a] however, recent ENDOR results on the cluster X indicate that one of the Fe sites has Fe(IV) character.[76b] Que and coworkers have isolated a $Fe_2(\mu\text{-oxo})_2$ species that is formally a valence-localized $S = {}^1/_2$ system, as confirmed by Mössbauer spectroscopy, and contains exchange-coupled high-spin Fe(IV) and Fe(III) sites.[77a] A similar complex with a slightly different version of a ligand produced a $S = {}^3/_2$ system with a Fe−Fe distance of 2.89 Å.[77b] A $Fe_2(III_2)$ site coupled to a ligand radical, or a valence-delocalized Fe_2(III,IV) center were both considered to explain the electronic parameters of the complex. Mössbauer spectra show that the Fe sites are equivalent and hence support a valence-delocalized high-spin $Fe_2(III,IV)(\mu\text{-oxo})_2$ site.

The Mn−Mn distance of ~2.9 Å in the S_3 state leads to our proposal that the oxidative equivalent is not stored on the Mn atoms but is substantially delocalized with significant charge and spin density on the bridging oxo ligand, generating a species akin to an oxyl radical. The presence of an unpaired electron on the oxygen will alter the $S = {}^1/_2$ ground spin state of the $Mn_4(III,IV_3)$ cluster. Thus this structure would provide a rationale for the disappearance of the multiline signal in the S_3-state samples. Mn is not oxidized during the S_2 to S_3 transition per se, because the oxidative equivalent is either predominantly localized on the oxygen atom or delocalized over the entire Mn_2O_2 unit; therefore, the observed lack of a concomitant change in the Mn K-edge position during the S_2 to S_3 transition. The increase in the Mn−Mn distance to 2.9 Å from 2.7 Å is in accord with that observed in the binuclear Fe complexes described above, where the Fe−Fe distance is 2.89 Å when the oxidative equivalent is delocalized on the $Fe_2(\mu\text{-oxo})_2$ unit.

Ca-depleted samples are inactive in O_2 evolution and a broad $g = 2$ EPR signal has been observed in the "S_3 state" of such samples. In such samples the $g = 2$ broadened EPR signal has been confirmed to arise from the tyrosine Y_Z radical, and it is proposed that the signal is broadened by interaction with the spin on the Mn cluster.[20] We propose that there is an equilibrium between the two states; one state is a radical residing on the oxo bridge, and the second state with the radical on the tyrosine Z residue. We propose that in Ca-depleted systems the equilibrium is shifted toward the stabilization of the tyrosine Y_Z radical and the oxidation of the oxo bridge is prevented. Ca and a neighboring residue are proposed to play a crucial role in controlling the redox potential and thus the stability and the course of the mechanism of water oxidation. This might explain the stability of the altered S_{2-}state multiline EPR signal in Ca-depleted samples and the inability to generate a regular MLS by illumination at 190 K in such samples.

Inhibitors like F^- or NH_3 prevent the formation of the delocalized S_3 state. In the case of NH_3 it is probably due to replacement of the oxo-bridge involved in oxidation by the amido group.

(4) We propose the formation of a di-oxyl radical species in the S_4 state. Formation of μ-η^2:η^2-peroxo intermediate from a di-μ-oxyl structure is an attractive possibility, based on recent reports involving a binuclear Cu complex,[78a,b] although no such Mn complex has yet been synthesized. The reverse reaction, homolysis of the O−O bond in a μ-η^2:η^2-peroxo structure to a di-μ-oxo core with attendant shortening of the intermetal distance from 3.5 to 2.8 Å was recently demonstrated for a binuclear Cu(II) complex.[78a] A more recent report shows that the two species are interconvertible by altering the solvent.[78b] We propose that the dioxyl radical−peroxo species spontaneously decomposes to form the S_0 state and O_2. The nature of the S_4 species proposed provides the reason for it being found only as a transient.

(5) On release of O_2, two hydroxy groups are incorporated into the binuclear Mn structure with concomitant release of two protons. Recent H/D isotope exchange data have been interpreted to include proton participation, probably breakage of H bonds, during electron abstraction from S_3 leading to O_2 formation.[79] The Mn−Mn distance in hydroxo-bridged structures is expected to be longer than 2.7 Å as hinted by data from an S_0 state generated by NH_2OH treatment.[30b] The presence of hydroxo bridges has a pronounced influence on the Mn−Mn exchange coupling. The lack of an EPR signal or the difficulty in detecting an EPR signal from the S_0 state could be related to a ground spin state that is not $S = {}^1/_2$.

The deprotonation steps occur early, during the S_0 to S_1 and S_1 to S_2 transitions, and this is consistent with the lack of proton hyperfine in the MLS. Water is incorporated as two hydroxide bridges (two protons are released during this transition) during the S_4 to S_0 transition when O_2 is released, and substrate water does not participate in the oxidation reactions until the S_3 state, bypassing the formation of potentially harmful water oxidation products. The mechanism also explains the asymmetry observed in the

exchangeable O atoms in the S_3 state. One of the oxygens is more similar to an oxyl radical while the other is an oxide which would exchange on a slower time scale. Renger et al. have proposed[79] that the H/D isotope effect observed for the S_3-S_4 transition can be rationalized if the substrate that is bound to Mn is hydrogen bonded and the cleavage of these bonds affects the rate constants. It is conceivable that an asymmetric configuration caused by H bonds to the oxo−oxyl intermediate in the S_3 state leads to the observed differences in $H_2{}^{18}O/H_2{}^{16}O$ exchange rates. Our proposed mechanism avoids the formation of the O−O bond until the most oxidized state is reached. This precludes the formation and release of peroxide or other oxidation products of water in the earlier S states, thus preventing the system from "short circuiting" and avoiding the risk of damaging the polypeptides of photosystem II.

VII. Conclusion

Our understanding of the structure of the Mn complex and the mechanism by which water is oxidized to dioxygen has grown considerably since the insightful hypothesis of the S-state intermediates by Kok[3a] more than two decades ago. Since then the development of pure and homogeneous oxygen evolving photosystem II preparations[12] has made possible the application of spectroscopic techniques, most notably electron paramagnetic resonance and X-ray absorption spectroscopy, to study the Mn complex as shown in this article.

Retrospectively, our first proposed model for charge storage that invoked the oxidation of a pair of Mn species from Mn(II) to Mn(IV) through S_0 to the S_4 states still has merit.[80] The evidence to date suggests that only two of the four Mn atoms in the cluster undergo reversible oxidation reduction.

In a review about the mechanism of photosynthetic water oxidation Renger[8a] set forth several questions and problems that needed to be addressed. There has been significant progress toward answering the questions, as shown in this article, but we note that many questions remain unanswered. What is the exact structure of the Mn complex? The structures derived from X-ray spectroscopy results, while topologically correct, might differ from a final resolved structure. What is the structural role of the obligatory cofactors Ca^{2+} and Cl^-? Almost nothing is known about the putative S_4 state; this state has not been trapped or otherwise detected. What are the oxidation states and the structure of the Mn cluster in the S_4 state? When and where do the water molecules or hydroxide species become incorporated? How are the oxygen atoms coupled to form an O−O bond? These questions, along with the need to trap and characterize the proposed transient S_4 state, offer challenges for the future; they need to be addressed before we can fully understand where and how plants oxidize water to dioxygen.

Acknowledgments

We thank Dr. Matthew Latimer, Dr. Annette Rompel, Roehl Cinco, Henk Visser, and John Robblee for their critical reading, help with preparation of this review, and the numerous discussions about every aspect of the proposals and interpretations presented in this review. We gratefully thank our present and former students, postdoctoral fellows and sabbatical visitors for their contributions to this effort. We thank our collaborators, Professors K. Wieghardt, G. Christou, W. H. Armstrong, J.-J. Girerd, and D. Hodgson for generously providing the Mn model complexes and sharing their considerable insight into the chemistry of Mn. We thank Professor V. L. Pecoraro for providing the Mn−Cl complexes. We are grateful to Professor L. Que, Jr. who brought to our attention the possibilities extant in Fe bioinorganic chemistry for explaining the data from the S_3 state. We thank Professor R. David Britt for providing us with his review on oxygen evolution prior to publication. This work was supported by the Director, Division of Energy Biosciences, Office of Basic Energy Sciences, U.S. Department of Energy (DOE) under contract DE-AC03-76SF00098. Synchrotron radiation facilities were provided by the Stanford Synchrotron Radiation Laboratory (SSRL) and the National Synchrotron Light Source (NSLS), both supported by DOE. The Biotechnology Laboratory at SSRL and Beam Line X9 at NSLS are supported by the National Center for Research Resources of the National Institutes of Health.

References

(1) (a) Pirson, A. *Z. Bot.* **1937**, *31*, 193−267. (b) For reviews, see: *Manganese Redox Enzymes*; Pecoraro, V. L., Ed; VCH Publishers: New York, 1992.

(2) For recent reviews of the OEC, see: (a) Debus, R. J. *Biochim. Biophys. Acta* **1992**, *1102*, 269−352. (b) Rutherford, A. W.; Zimmermann, J.-L.; Boussac, A. In *The Photosystems: Structure, Function, and Molecular Biology*; Barber, J., Ed.; Elsevier: Amsterdam, 1992; pp 179−229. (c) Hansson, Ö.; Wydrzynski, T. *Photosyn. Res.* **1990**, *23*, 131−162. (d) Andréasson, L.-E.; Vänngård, T. *Annu. Rev. Plant Physiol. Plant Mol. Biol.* **1988**, *39*, 379−411. (e) Babcock, G. T. In *New Comprehensive Biochemistry in Photosynthesis*; Amesz, J., Ed.; Elsevier: Amsterdam, 1987; Vol. 15, pp 125−158. (f) Britt, R. D. In *Oxygenic Photosynthesis: The Light Reactions*; Ort, D. R., Yocum, C. F., Eds.; Kluwer Academic Publishers: Dordrecht, 1996; pp 137−164.

(3) (a) Kok, B.; Forbush, B.; McGloin, M. *Photochem. Photobiol.* **1970**, *11*, 457−475. (b) Joliot, B.; Barbieri, G.; Chabaud, R. *Photochem. Photobiol.* **1969**, *10*, 309−329.

(4) (a) Yocum C. F. In *Manganese Redox Enzymes*; Pecoraro, V. L., Ed.; VCH Publishers: New York, 1992; pp 71−83. (b) Yocum C. F. *Biochim. Biophys. Acta* **1991**, *1059*, 1−15. (c) Homann, P. H *J. Bioenerg. Biomembr.* **1987**, *19*, 105−123. (d) Coleman, W. J. *Photosynth. Res.* **1990**, *23*, 1−27.

(5) Renger, G. In *Photosynthetic Oxygen Evolution*; Metzner, H., Ed.; Academic Press: London, 1978; pp 229−248.

(6) (a) Sauer, K.; Yachandra, V. K.; Britt, R. D.; Klein, M. P. In *Manganese Redox Enzymes*; Pecoraro, V. L., Ed.; VCH Publishers: New York, 1992; pp 141−175. (b) Klein, M. P.; Sauer, K.; Yachandra, V. K. *Photosynth. Res.* **1993**, *38*, 265−277.

(7) (a) Brudvig, G. W. In *Advanced EPR: Applications in Biology and Biochemistry*; Hoff, A. J. Ed.; Elsevier: Amsterdam, 1990; pp 839−865. (b) Vänngård, T.; Hansson, Ö.; Haddy, A. In *Manganese Redox Enzymes*; Pecoraro, V. L., Ed.; VCH Publishers: New York, 1992; pp 105−118.

(8) (a) Renger, G. *Photosynthetica* **1987**, *21*, 203−224. (b) Kambara, T.; Govindjee *Proc. Natl. Acad. Sci. USA* **1985** *82*, 6119−6123.

(9) (a) Wieghardt, K. *Angew. Chem., Int. Ed. Engl.* **1989**, *28*, 1153−1172. (b) Pecoraro, V. L. *Photochem. Photobiol.* **1988**, *48*, 249−264. (c) Christou, G. *Acc. Chem. Res.* **1989**, *22*, 328−335. (d) Armstrong, W. H. In *Manganese Redox Enzymes*; Pecoraro, V. L., Ed.; VCH: New York, 1992; pp 261−286. (e) Pecoraro, V. L. In *Manganese Redox Enzymes*; Pecoraro, V. L., Ed.; VCH: New York, 1992; pp 197−232. (f) Pecoraro, V. L.; Baldwin, M. J.; Gelasco, A. *Chem. Rev.* **1994**, *94*, 807−826.

(10) (a) Deisenhofer, J.; Michel, H. *Biochemistry* **1988**, *27*, 1−7. (b) Trebst, A.; Depka, B. In *Antennas and Reaction Centers of Photosynthetic Bacteria - Structure, Interactions and Dynamics*; Michel-Beyerle, M. E., Ed.; Springer-Verlag: Berlin, 1985; pp

216−224. (c) Youvan, D. C.; Bylina, E. J.; Alberti, M.; Begusch, H.; Hearst, J. E. *Cell* **1984**, *37*, 949−957. (d) Hearst, J. E. *Encyl. Plant Physiol., New Ser.* **1986**, *19*, 382−389. (e) Hearst, J. E.; Sauer, K. *Z. Naturforsch.* **1984**, *39c*, 421−424. (f) Mathis, P.; Rutherford, A. W. In *New Comprehensive Biochemistry in Photosynthesis*; Amesz, J., Ed.; Elsevier: Amsterdam, 1987; Vol. 15, pp 63−96.

(11) (a) Pakrasi, J. B.; Vermaas, W. F. J. In *The Photosystems: Structure, Function, and Molecular Biology*; Barber, J., Ed.; Elsevier: Amsterdam, 1992; pp 231−257. (b) Chu, H. A.; Nguyen, A. P.; Debus, R. J. *Biochemistry* **1995**, *34*, 5839−5858. (c) Chu, H. A.; Nguyen, A. P.; Debus, R. J. *Biochemistry* **1995**, *34*, 5859−5882. (d) Nixon, P. J.; Diner, B. A. *Biochem. Soc. Trans.* **1994**, *22*, 338−343. (e) Nixon, P. J.; Chisholm, D. A.; Diner, B. A. In *Plant Protein Engineering*; Cambridge University Press: Cambridge, 1992; pp 93−141.

(12) (a) Berthold, D. A.; Babcock, G. T.; Yocum, C. F. *FEBS Lett.* **1981**, *134*, 231−234. (b) Kuwabara ,T.; Murata, N. *Plant Cell Physiol.* **1982**, *23*, 533−539.

(13) (a) Ghanotakis, D. F.; Demetrious, D. M.; Yocum, C. F. *Biochim. Biophys. Acta* **1987**, *891*, 15−21. (b) Adir, N.; Okamura, M. Y.; Feher, G. In *Research in Photosynthesis*; Murata, N., Ed.; Kluwer: Dordrecht, 1992; Vol. II, pp 195−198.

(14) (a) Satoh, K.; Ohno, T.; Katoh, *FEBS Lett.* **1985**, *180*, 326−330. (b) Noren, G. H.; Boerner, R. J.; Barry, B. A. *Biochemistry* **1991**, *30*, 3943−3950. (c) Kirilovsky, D. L.; Boussac, A. G. P.; van Mieghem, F. J. E.; Ducruet, J.-M. R. C.; Sétif, P. R.; Yu, J.; Vermaas, W. F. J.; Rutherford, A. W. *Biochemistry* **1992**, *31*, 2099−2107. (d) Tang, X. S.; Diner, B. A. *Biochemistry* **1994**, *33*, 4594−4603.

(15) (a) Dismukes, G. C.; Siderer, Y. *Proc. Natl. Acad. Sci. USA* **1981**, *78*, 274−278. (b) Cooper, S. R.; Dismukes, G. C.; Klein, M. P.; Calvin, M. *J. Am. Chem. Soc.* **1978**, *100*, 7248−7252. (c) Dismukes, G. C.; Ferris, K.; Watnick, P. *Photobiochem. Photobiophys.* **1982**, *3*, 243−256. (d) Hansson, Ö.; Andréasson, L.-E. *Biochim. Biophys. Acta* **1982**, *679*, 261−268. (e) Plaksin, P. M.; Stoufer, R. C.; Mathew, M.; Palenik, G. J. *J. Am. Chem. Soc.* **1971**, *94*, 2121−2122.

(16) (a) Casey, J. L.; Sauer, K. *Biochim. Biophys. Acta* **1984**, *767*, 21−28. (b) Zimmermann, J.-L.; Rutherford, A. W. *Biochim. Biophys. Acta* **1984**, *767*, 160−167. (c) Zimmermann, J.-L.; Rutherford, A. W. *Biochemistry* **1986**, *25*, 4609−4615.

(17) (a) Hansson, Ö.; Aasa, R.; Vänngård, T. *Biophys. J.* **1987**, *51*, 825−832. (b) de Paula, J. C.; Brudvig, G. W. *J. Am. Chem. Soc.* **1985**, *107*, 2643−2648. (c) Haddy, A.; Dunham, W. R.; Sands, R. H.; Aasa, R. *Biochim. Biophys. Acta* **1992**, 1099, 25−34.

(18) (a) Boussac, A.; Zimmermann, J.-L.; Rutherford, A. W. *Biochemistry* **1989**, *28*, 8984−8989. (b) Sivaraja, M.; Tso, J.; Dismukes, G. C. *Biochemistry* **1989**, *28*, 9459−9464.

(19) Boussac, A.; Zimmermann, J.-L.; Rutherford, A. W.; Lavergne, J. *Nature* **1990**, *347*, 303−306.

(20) Gilchrist, M. I.; Ball, J. A.; Randall, D. W.; Britt, R. D. *Proc. Natl. Acad. Sci. USA* **1995**, *92*, 9545−9549.

(21) (a) Dexheimer, S. L.; Klein, M. P. *J. Am. Chem. Soc.* **1992**, *114*, 2821−2826. (b) Dexheimer, S. L.; Gohdes, J. W.; Chan, M. K.; Hagen, K. S.; Armstrong, W. H.; Klein, M. P. *J. Am. Chem. Soc.* **1989**, *111*, 8923−8925.

(22) Koulougliotis, D.; Hirsh, D. J.; Brudvig, G. W. *J. Am. Chem. Soc.* **1992**, *114*, 8322−8323.

(23) Sharp, R. R. In *Manganese Redox Enzymes*; Pecoraro, V. L., Ed.; VCH Publishers: New York, 1992; pp 177−196.

(24) (a) Styring, S. A.; Rutherford, A. W. *Biochemistry* **1988**, *27*, 4915−4923. (b) Evelo, R. G.; Styring, S.; Rutherford, A. W.; Hoff, A. J. *Biochim. Biophys. Acta* **1989**, *973*, 428−442.

(25) (a) Kirby, J. A.; Goodin, D. B.; Wydrzynski, T.; Robertson, A. C.; Klein, M. P. *J. Am. Chem. Soc.* **1981**, *103*, 5537−5542. (b) Cramer, S. P.; Eccles, T. K.; Kutzler, F.; Hodgson, K. O.; Mortenson, L. E. *J. Am. Chem. Soc.* **1976**, *98*, 1287−1288. (c) Sauer, K.; Guiles, R. D.; McDermott, A. E.; Cole, J. L.; Yachandra, V. K.; Zimmermann, J.-L.; Klein, M. P.; Dexheimer, S. L.; Britt, R. D. *Chem. Scr.* **1988**, *28A*, 87−91.

(26) (a) Goodin, D. B.; Yachandra, V. K.; Britt, R. D.; Sauer, K.; Klein, M. P. *Biochim. Biophys. Acta* **1984**, *767*, 209−216. (b) McDermott, A. E.; Yachandra, V. K.; Guiles, R. D.; Cole, J. L.; Dexheimer, S. L.; Britt, R. D.; Sauer, K.; Klein, M. P. *Biochemistry* **1988**, *27*, 4021−4031. (c) Yachandra, V. K.; Guiles, R. D.; McDermott, A. E.; Cole, J. L.; Britt, R. D.; Dexheimer, S. L.; Sauer, K.; Klein, M. P. *Biochemistry* **1987**, *26*, 5974−5981. (d) Cole, J. L.; Yachandra ,V. K.; Guiles, R. D.; McDermott, A. E.; Britt, R. D.; Dexheimer, S. L.; Sauer, K.; Klein, M. P. *Biochim. Biophys. Acta* **1987**, *890*, 395−398 (e) DeRose, V. J. Ph.D. Dissertation, University of California, Berkeley, 1990; Lawrence Berkeley Laboratory Report, LBL-30077.

(27) Yachandra, V. K.; DeRose, V. J.; Latimer, M. J.; Mukerji, I.; Sauer, K.; Klein, M. P. In *Research in Photosynthesis*; Murata, N., Ed.; Kluwer: Dordrecht, 1992; Vol. II, pp 281−287.

(28) (a) Ono, T.; Noguchi, T.; Inoue, Y.; Kusunoki, M.; Matsushita, T.; Oyanagi, H. *Science* **1992**, *258*, 1335−1337. (b) Penner-Hahn, J. E.; Fronko, R. M.; Pecoraro, V. L.; Yocum, C. F.; Betts, S. D.; Bowlby, N. R. *J. Am. Chem. Soc.* **1990**, *112*, 2549−2557. (c) Riggs, P. J.; Mei, R.; Yocum, C. F.; Penner-Hahn, J. E. *J. Am. Chem. Soc.* **1992**, *114*, 10650−10651.

(29) (a) Baldwin, M. J.; Stemmler, T. L.; Riggs-Gelasco, P. J.; Kirk, M. L.; Penner-Hahn, J.-E.; Pecoraro, V. L. *J. Am. Chem. Soc.* **1994**, *116*, 11349−11356. (b) Larson, E. J.; Riggs, P. J.; Penner-Hahn, J. E.; Pecoraro, V. L. *J. Chem. Soc., Chem. Commun.* **1992**, 102−103.

(30) (a) Guiles, R. D.; Zimmermann, J.-L.; McDermott, A. E.; Yachandra, V. K.; Cole, J. L.; Dexheimer, S. L.; Britt, R. D.; Wieghardt, K.; Bossek, U.; Sauer, K.; Klein, M. P. *Biochemistry* **1990**, *29*, 471−485. (b) Guiles, R. D.; Yachandra, V. K.; McDermott, A. E.; Cole, J. L.; Dexheimer, S. L.; Britt, R. D.; Sauer, K.; Klein, M. P. *Biochemistry* **1990**, *29*, 486−496.

(31) Roelofs, T. A.; Liang, W.; Latimer, M. J.; Cinco, R. M.; Rompel, A.; Andrews, J. C.; Sauer, K.; Yachandra, V. K.; Klein, M. P. *Proc. Natl. Acad. Sci. USA* **1996**, *93*, 3335−3340.

(32) (a) Dekker, J. In *Manganese Redox Enzymes*; Pecoraro, V. L., Ed.; VCH Publishers: New York, 1992; pp 85−103. (b) Haumann, M., Drevenstedt, W.; Hundelt, M.; Junge, W. *Biochim. Biophys. Acta* **1996**, *1273*, 237−250.

(33) (a) de Paula, J. C.; Beck, W. F.; Brudvig, G. W. *J. Am. Chem. Soc.* **1986**, *108*, 4002−4009. (b) Britt, R. D.; Lorigan, G. A.; Sauer, K.; Klein, M. P.; Zimmermann, J.-L. *Biochim. Biophys. Acta* **1992**, *1040*, 95−101. (c) Lorigan, G. A.; Britt, R. D. *Biochemistry* **1994**, *33*, 12072−12076.

(34) (a) Kim, D. H.; Britt, R. D.; Klein, M. P.; Sauer, K. *J. Am. Chem. Soc.* **1990**, *112*, 9389−9391. (b) Kim, D. H.; Britt, R. D.; Klein, M. P.; Sauer, K. *Biochemistry* **1992**, *31*, 541−547. (c) Smith, P. J.; Pace, R. J. In *Photosynthesis: From Light to Biosphere*; Mathis, P., Ed.; Kluwer: Netherlands, 1995; Vol. II, pp 317−320.

(35) Boussac, A.; Girerd, J.-J; Rutherford, A. W. *Biochemistry* **1996**, *35*, 6984−6989.

(36) (a) Bonvoisin, J.; Blondin, G.; Girerd, J.-J.; Zimmermann, J.-L. *Biophys. J.* **1992**, *61*, 1076−1086. (b) Zheng, M.; Dismukes, G. C. In *Research in Photosynthesis*; Murata, N., Ed.; Kluwer Publishers: Dordrecht, Netherlands, 1992; Vol. II, pp 305−308. (c) Kusunoki, M. *Chem. Phys. Lett.* **1992**, *197*, 108−116. (d) Ahrling, K.; Pace, R. J. *Biophys. J.* **1995**, *68*, 2081−2090.

(37) (a) Yachandra, V. K.; Guiles, R. D.; Sauer, K.; Klein, M. P. *Biochim. Biophys. Acta* **1986**, *850*, 333−342. (b) Haddy, A.; Aasa, R.; Andréasson, L.-E. *Biochem*istry **1989**, *28*, 6954−6959.

(38) Randall, D. W.; Sturgeon, B. E.; Ball, J. A.; Lorigan, G. A.; Chan, M. K.; Klein, M. P.; Armstrong, W. H.; Britt, R. D. *J. Am. Chem. Soc.* **1995**, *117*, 11780−11789.

(39) (a) Yachandra, V. K., Klein, M. P. In *Biophysical Techniques in Photosynthesis, Advances in Photosynthesis*; Amesz, J., Hoff, A. J., Eds.; Kluwer Publishers: Dordrecht, Netherlands, 1996; Vol. 3, pp 337−354. (b) Yachandra, V. K. In *Biochemical Spectroscopy, Methods in Enzymology*; Sauer, K., Ed.; Academic Press: Orlando, FL, 1995; Vol. 246, pp 638−675. (c) Cramer, S. P. In *X-ray Absorption: Principles, Applications, and Techniques of EXAFS, SEXAFS, and XANES;* Koningsberger, D. C., Prins, R., Eds.; Wiley-Interscience: New York, 1988; pp 257−320. (d) Scott, R. A. In *Methods Enzymology*; Academic Press: Orlando, FL, 1985; Vol. 107, pp 414−459. (e) Powers, L. *Biochim. Biophys. Acta* **1982**, *683*, 1−38. (f) Lee, P. A.; Citrin, P. H.; Eisenberger, P.; Kincaid, B. M. *Rev. Mod. Phys.* **1981**, *53*, 769−806.

(40) Kirby, J. A.; Robertson, A. S.; Smith, J. P.; Cooper, S. R.; Klein, M. P. *J. Am. Chem. Soc.* **1981**, ***103***, 5529−5537.

(41) Yachandra, V. K.; Guiles, R. D.; McDermott, A. E.; Britt, R. D.; Dexheimer, S. L.; Sauer, K.; Klein, M. P. *Biochim. Biophys. Acta* **1986**, *850*, 324−332.

(42) Cole, J. L.; Yachandra, V. K.; McDermott, A. E.; Guiles, R. D.; Britt, R. D.; Dexheimer, S. L.; Sauer, K.; Klein, M. P. *Biochemistry* **1987**, *26*, 5967−5973.

(43) For reviews of the Mn−O/N distances in multinuclear Mn complexes see refs 1b and 9 and references therein.(a) Wieghardt, K.; Bossek, U.; Ventur, D.; Weiss, J. *J. Chem. Soc., Chem. Commun.* **1985,** 347−349. (b) Vincent, J. B.; Chang, H.-R.; Folting, K.; Huffman, J. C.; Christou, G.; Hendrickson, D. N. *J. Am. Chem. Soc.* **1987**, *109*, 5703−5711. (c) Christou, G.; Vincent, J. B. *Metal Clusters in Proteins*; Que, L., Ed; ACS Symp. Ser. 372; American Chemical Society: Washington, DC, 1988; pp 238−255. (d) Auger, N.; Girerd, J.-J.; Corbella, M.; Gleizes, A.; Zimmermann, J.-L. *J. Am. Chem. Soc.* **1990**, *112*, 448−450. (e) Vincent, J. B.; Christmas, C.; Huffman, J. C.; Christou, G.; Chang, H.-R.; Hendrickson, D. N. *J. Chem. Soc., Chem. Commun.* **1987**, 236−238. (f) Wang, S.; Folting, K.; Streib, W. E.; Schmitt, E. A.; McCusker, J. K.; Hendrickson, D. N.; Christou, G. *Angew. Chem., Int. Ed. Engl.* **1991**, *30* , 305−306.

(44) For comprehensive reviews of the Mn−Mn distances in multinuclear Mn complexes see refs 1b and 9 and references therein. Also see (ref 43). A representative, but not a complete, list of references is listed here. (a) Stebler, M.; Ludi, A.; Burgi, H.-B. *Inorg. Chem.* **1986**, *25*, 4743−4750. (b) Wieghardt, K.; Bossek, U.; Zsolnai, L.; Huttner, G., Blondin, G.; Girerd, J. J.; Babonneau, F. *J. Chem. Soc., Chem. Commun.* **1987**, 651−653. (c) Wieghardt, K.; Bossek, U.; Nuber, B.; Weiss, J.; Bonvoisin, J.; Corbella, M.; Vitols, S. E.; Girerd, J. J. *J. Am. Chem. Soc.* **1988**,

110, 7398−7411. (d) Christmas, C.; Vincent, J. B.; Huffman, J. C.; Christou, G.; Chang, H.-R.; Hendrickson, D. N. *J. Chem. Soc., Chem. Commun.* **1987**, 1303−1305. (e) Bashkin, J. S.; Chang, H.-R.; Streib, W. E.; Huffman, J. C.; Hendrickson, D. N.; Christou, G. *J. Am. Chem. Soc.* **1987**, *109*, 6502−6504. (f) Sheats, J. E.; Czernuszewicz, R. S.; Dismukes, G. C.; Rheingold, A. L.; Petrouleas, V.; Stubbe, J.; Armstrong, W. H.; Beer, R. H.; Lippard, S. J. *J. Am. Chem. Soc.* **1987**, *109*, 1435−1444. (g) Wieghardt, K.; Bossek., U.; Bonvoisin, J.; Beauvillain, P.; Girerd, J.-J.; Nuber, B.; Weiss, J.; Heinze, J. *Angew. Chem.* **1986**, *98*, 1026−1027. (h) Wieghardt, K.; Bossek, U.; Gebert, W. *Angew. Chem.* **1983**, *95*, 320 (i) Hagen, K. S.; Armstrong, W. H.; Hope, H. *Inorg. Chem.* **1988**, *27*, 967−969. (j) Collins, M. A.; Hodgson, D. J.; Michelsen, K.; Towle, D. K. *J. Chem. Soc., Chem. Commun.* **1987**, 1659−1660. (k) Towle, D. K.; Botsford, C. A.; Hodgson, D. J. *Inorg. Chim. Acta* **1988**, *141*, 167−168. (l) Suzuki, M.; Tokura, S.; Suhara, M.; Uehara, A. *Chem. Lett.* **1988**, 477−480. (m) Goodson, P. A.; Hodgson, D. J. *Inorg. Chem.* **1989**, *28*, 3606−3608. (n) Libby, E.; Webb, R. J.; Streib, W. E.; Folting, K.; Huffman, J. C.; Hendrickson, D. N.; Christou, G. *Inorg. Chem.* **1989**, *28*, 4037−4040. (o) Brewer, K. J.; Liegeois, A.; Otvos, J. W.; Calvin, M.; Spreer, L. O. *J. Chem. Soc., Chem. Commun.* **1988**, 1219−1220. (p) Suzuki, M.; Senda, H.; Kobayashi, Y.; Oshio, H.; Uehara, A. *Chem. Lett.* **1988**, 1763−1766. (q) Goodson, P. A.; Glerup, J.; Hodgson, D. J.; Michelsen, K.; Pedersen, E. *Inorg. Chem.* **1990**, *29*, 503−508. (r) Brewer, K. J.; Calvin, M.; Lumpkin, R. S.; Otvos, J. W.; Spreer, L. O. *Inorg. Chem.* **28**, 4446−4451. (s) Oki, A. R.; Glerup, J.; Hodgson, D. J. *Inorg. Chem.* **1990**, *29*, 2435−2441. (t) Glerup, J.; Goodson, P. A.; Hazell, A.; Hazell, R.; Hodgson, D. J.; McKenzie, C. J.; Michelsen, K.; Rychlewska, U.; Toftlund. *Inorg. Chem.* **1994**, *33*, 4105−4111.

(45) Scott, R. A.; Eidsness, M. K. *Comments Inorg. Chem.* **1988**, *7*, 235−267.

(46) (a) MacLachlan, D. J.; Hallahan, B. J.; Ruffle, S. V.; Nugent, J. H. A.; Evans, M. C. W.; Strange, R. W.; Hasnain, S. S. *Biochem. J.* **1992**, *285*, 569−576. (b) DeRose, V. J.; Mukerji, I.; Latimer, M. J.; Yachandra, V. K.; Sauer, K.; Klein, M. P. *J. Am. Chem. Soc.* **1994**, *116*, 5239−5249. (c) Yachandra, V. K.; DeRose, V. J.; Latimer, M. J.; Mukerji, I.; Sauer, K.; Klein, M. P. *Science* **1993**, *260*, 675−679.

(47) (a) George, G. N.; Prince, R. C.; Cramer, S. P. *Science* **1989**, *243*, 789−791. (b) Mukerji, I.; Andrews, J. C.; DeRose, V. J.; Latimer, M. J.; Yachandra, V. K.; Sauer, K.; Klein, M. P. *Biochemistry* **1994**, *33*, 9712−9721.

(48) (a) Vincent, J. B.; Christou, G. *Inorg. Chim. Acta* **1987**, *136*, L41−L43. (b) Philouze, C.; Blondin, G.; Menage, S.; Auger, N.; Girerd, J.-J.; Vigner, D.; Lance, M.; Nierlich, M. *Angew. Chem., Int. Ed. Engl.* **1992**, *31*, 1629−1631. (c) Chan, M. K.; Armstrong, W. H. *J. Am. Chem. Soc.* **1991**, 113, 5055−5057. (d) Kirk, M. L.; Chan, M. K.; Armstrong, W. H.; Solomon, E. I. *J. Am. Chem. Soc.* **1992**, *114*, 10432−10440. (e) Low, D. W.; Eichhorn, D. M.; Dragenescu, A.; Armstrong, W. H. *Inorg. Chem.* **1991**, *30*, 877−878. (f) McKee, V.; Tandon, S. S. *J. Chem. Soc., Chem. Commun.* **1988**, 1334−1336. (g) Proserpio, D. M.; Hoffmann, R.; Dismukes, G. C. *J. Am. Chem. Soc.* **1992**, *114*, 4374−4382. (h) Philouze, C.; Blondin, G.; Girerd, J.-J.; Guilhem, J.; Pascard, C.; Klein, M. *J. Inorg. Biochem.* **1993**, *282*, D015.

(49) Chen, C. G.; Kazimir, J.; Cheniae, G. M. *Biochemistry* **1995**, *34*, 13511−13526.

(50) (a) Ghanotakis, D. F.; Babcock, G. T.; Yocum, C. F. *FEBS Lett.* **1984**, *167*, 127−130. (b) Boussac, A.; Rutherford, A. W. *Biochemistry* **1988**, *27*, 3476−3483.

(51) (a) Boussac, A.; Zimmermann, J.-L.; Rutherford, A. W. *FEBS Lett.* **1990**, *277*, 69−74. (b) Zimmermann, J.-L.; Boussac, A.; Rutherford, A. W. *Biochemistry* **1993**, *32*, 4831−4841. (c) van Vliet, P.; Boussac, A.; Rutherford, A. W. *Biochemistry* **1994**, *33*, 12998−13004.

(52) (a) Latimer, M. J.; DeRose, V. J.; Mukerji, I.; Yachandra, V. K.; Sauer, K.; Klein, M. P. *Biochemistry* **1995**, *34*, 10898−10909. (b) Latimer M. J. Ph.D. Dissertation, University of California, Berkeley, 1995; Lawrence Berkeley Laboratory Report, LBL-37897. (c) Ono, T.-A.; Kusunoki, M.; Matsushita, T.; Oyanagi, H.; Inoue, Y. *Biochemistry* **1991**, *30*, 6836−6841.

(53) (a) Penner-Hahn, J. E.; Riggs-Gelasco, P. J.; Yu, E.; DeMarois, P.; Yocum, C. F. In *Photosynthesis: From Light to Biosphere*; Mathis, P., Ed.; Kluwer: Netherlands, 1995; pp 241−246. (b) Riggs-Gelasco, P. J.; Mei, R.; Ghanotakis, D. F.; Yocum, C. F.; Penner-Hahn, J. E. *J. Am. Chem. Soc.* **1996**, *118*, 2400−2410.

(54) (a) van Vliet, P.; Rutherford, A. W. *Biochemistry* **1996**, *35*, 1829−1839. (b) Rashid, A.; Homann, P. H. *Biochim. Biophys. Acta* **1992**, *1101*, 303−310.

(55) Lindberg, K.; Vänngård, T.; Andréasson, L.-E. *Photosynth. Res.* **1993**, *38*, 401−408.

(56) (a) Ono, T.; Zimmermann, J.-L.; Inoue, Y.; Rutherford, A. W. *Biochim. Biophys. Acta* **1986**, *851*, 193−201. (b) Ono, T.-A.; Noguchi, T.; Inoue, Y.; Kusunoki, M.; Yamaguchi, H.; Oyanagi, H. *J. Am. Chem. Soc.* **1995**, *117*, 6386−6387.

(57) Boussac, A. L. *Chem. Phys.* **1995**, *194*, 409−418.

(58) (a) DeRose, V. J.; Latimer, M. J.; Zimmermann, J.-L.; Mukerji, I.; Yachandra, V. K.; Sauer, K.; Klein, M. P. *Chem. Phys.* **1995**, *194*, 443−459. (b) Kusunoki, M. In *Research in Photosynthesis*; Murata, N., Ed.; Kluwer: Dordrecht, 1992; Vol. II, pp 297−300.

(59) Nixon, P. J.; Diner, B. A. *Biochemistry* **1992**, *31*, 942−948.

(60) Noguchi, T.; Ono, T.-A.; Inoue, Y. *Biochim. Biophys. Acta* **1995**, *1228*, 189−200.

(61) (a) DeRose, V. J.; Yachandra, V. K.; McDermott, A. E.; Britt, R. D.; Sauer, K.; Klein, M. P. *Biochemistry* **1991**, *30*, 1335−1341. (b) Tang, X. S.; Diner, B. A.; Larsen, B. S.; Gilchrist, M. L.; Lorigan, G. A.; Britt, R. D. *Proc. Natl. Acad. Sci. USA* **1994**, *91*, 704−708.

(62) (a) Beck, W. F.; de Paula, J. C.; Brudvig, G. W. *J. Am. Chem. Soc.* **1986**, *108*, 4018−4022. (b) Britt, R. D., Zimmermann, J.-L., Sauer, K.; Klein, M. P. *J. Am. Chem. Soc.* **1989**, *111*, 3522−3532.

(63) Liang, W.; Latimer, M. J.; Dau, H.; Roelofs, T. A.; Yachandra, V. K.; Sauer, K.; Klein, M. P. *Biochemistry* **1994**. *33*, 4923−4932.

(64) Dau, H.; Andrews, J. C.; Roelofs, T. A.; Latimer, M. J.; Liang, W.; Yachandra, V. K.; Sauer, K.; Klein, M. P. *Biochemistry* **1995**, *34*, 5274−5287.

(65) Liang, W.; Roelofs, T. A.; Olsen, G. T.; Latimer, M. J.; Cinco, R. M.; Rompel, A.; Sauer, K.; Yachandra, V. K.; Klein, M. P. In *Photosynthesis: From Light to Biosphere*; Mathis, P., Ed.; Kluwer: Netherlands, 1995; pp 413−416.

(66) Baldwin, M. J.; Gelasco, A.; Pecoraro, V. L. *Photosynth. Res.* **1993**, *38*, 303−30.

(67) Renger, G. *Angew. Chem., Int. Ed. Engl.* **1987**, *26*, 643−660.

(68) Brudvig, G. W.; Crabtree, R. H. *Proc. Natl. Acad. Sci. USA* **1986**, *83*, 4586−4588.

(69) (a) Bossek, U.; Weyermüller, T.; Wieghardt, K.; Nuber, B.; Weiss, J. *J. Am. Chem. Soc.* **1990**, *112*, 6387−6388. (b) Bhula, R.; Gainsford, G. J.; Weatherburn, D. C. *J. Am. Chem. Soc.* **1988**, *110*, 7550−7552. (c) Kitajima, N.; Komatsuzaki, H.; Hikichi, S.; Osawa, M.; Moro-oka, Y. *J. Am. Chem. Soc.* **1994**, *116*, 11596−11597.

(70) (a) Krishtalik, L. I. *Biochim. Biophys. Acta* **1986**, *849*, 162−171. (b) Brudvig, G. W.; de Paula, J. In *Progress in Photosynthesis Research*; Biggins, J., Ed.; Martinus Nijhoff: The Hague, 1987; Vol. I, pp 490−498.

(71) Hansson, Ö.; Andréasson, L.-E.; Vänngård, T. *FEBS Lett.* **1987**, *195*, 151−154.

(72) Britt, R. D. Ph.D. Dissertation, University of California, Berkeley, 1988; LBL-Report 25042.

(73) (a) Radmer, R.; Ollinger, O. *FEBS Lett.* **1983**, *152*, 39−43. (b) Radmer, R.; Ollinger, O. *FEBS Lett.* **1986**, *195*, 285−289. (c) Messinger, J.; Badger, M.; Wydrzynski, T. *Proc. Natl. Acad. Sci. USA* **1995**, *92*, 3209−3213.

(74) Christou, G.; Vincent, J. B. *Biochim. Biophys. Acta* **1987**, *895*, 259−274.

(75) Hoganson, C. W.; Lydakis-Simantiris, N.; Tang, X.-S.; Tommos, C.; Warncke, K.; Babcock, G. T.; Diner, B. A.; McCracken, J.; Styring, S. *Photosynth. Res.* **1995**, *46*, 177−184.

(76) (a) Ravi, N.; Bollinger, J. M.; Huynh, B. H.; Edmondson, D. E.; Stubbe, J. *J. Am. Chem. Soc.* **1994**, *116*, 8007−8014. (b) Burdi, D.; Sturgeon, B. E.; Tong, W. H.; Stubbe, J.; Hoffman, B. M. *J. Am. Chem. Soc.* **1996**, *118*, 281−282.

(77) (a) Dong, Y.; Que, L., Jr.; Kauffmann, K.; Münck, E. *J. Am. Chem. Soc.* **1995**, *117*, 11377−11378. (b) Dong, Y.; Fujii, H.; Hendrich, M. P.; Leising, R. A.; Pan, G.; Randall, C. R.; Wilkinson, E. C.; Zang, Y.; Que, L., Jr.; Fox, B. G.; Kauffmann, K.; Münck, E. *J. Am. Chem. Soc.* **1995**, *117*, 2778−2792.

(78) (a) Mahapatra, S.; Halfen, J. A.; Wilkinson, E. C.; Pan, G.; Cramer, C. J.; Que, L.; Tolman, W. B. *J. Am. Chem. Soc.* **1995**, *117*, 8865−8866. (b) Halfen, J. A.; Mahapatra, S.; Wilkinson, E. C.; Kaderli, S.; Young, V. G., Jr.; Que, L., Jr.; Zuberbühler, A. D.; Tolman, W. B. *Science* **1996**, *271*, 1397−1400.

(79) Karge, M.; Irrgang, K.-D.; Sellin, S.; Feinäugle, R.; Liu, B.; Eckert, H.-J.; Eichler, H. J.; Renger, G. *FEBS Lett.* **1996**, *378*, 140−144.

(80) Blankenship, R. E. Ph.D. Dissertation, University of California, Berkeley, CA, 1974; Lawrence Berkeley Laboratory Report, LBL-3679.

CR950052K